Lignin

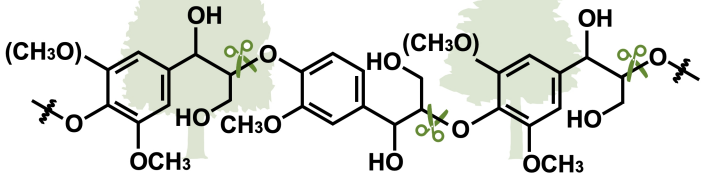

Cleavage of β-aryl ether linkages

: DDQ/*t*BuONO/O_2, Zn

Chemical depolymerization

Microbial conversion Engineered *Pseudomonas putida*

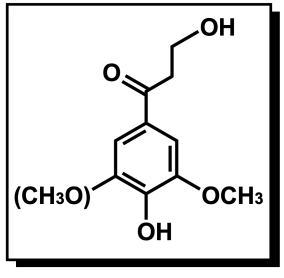

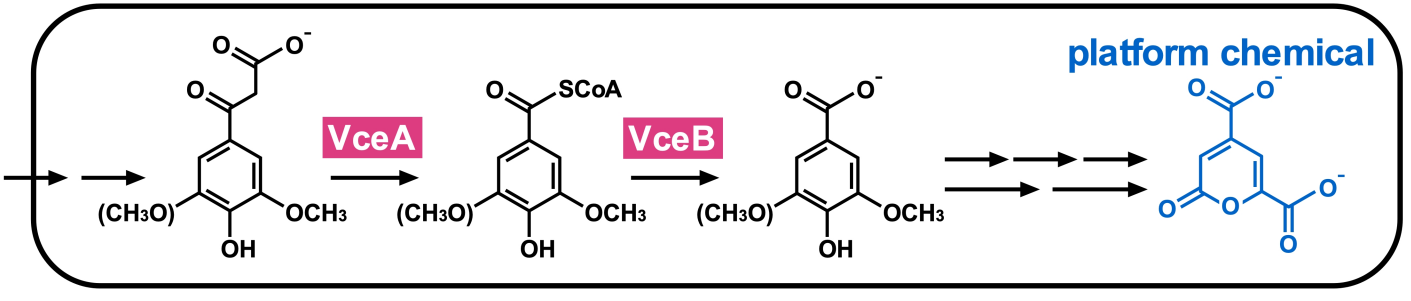

Highlights

- We identified and characterized two novel genes encoding an acetyl-CoA-dependent β-keto acid cleavage enzyme specific for the metabolites of arylglycerol-β-aryl ether [vanilloyl acetic acid/3-(4-hydroxy-3,5-dimethoxyphenyl)-3-oxopropanoic acid] and a vanilloyl-CoA/syringoyl-CoA thioesterase from *Sphingobium* sp. strain SYK-6.
- We designed a metabolic pathway to convert β-hydroxypropiovanillone to a platform chemical, 2-pyrone-4,6-dicarboxylate.
- We proposed a novel lignin valorization strategy by combining a chemical process that produces β-hydroxypropiovanillone/β-hydroxypropiosyringone from lignin with microbial catabolic functions.

Discovery of novel enzyme genes involved in the conversion of an arylglycerol-β-aryl ether metabolite and their use in generating a metabolic pathway for lignin valorization

Yudai Higuchi[a], Ryo Kato[a], Koichiro Tsubota[a], Naofumi Kamimura[a], Nicholas J. Westwood[b], and Eiji Masai[a*]

[a]Department of Bioengineering, Nagaoka University of Technology, Nagaoka, Niigata, Japan

[b]School of Chemistry and Biomedical Sciences Research Complex, University of St Andrews and EaStCHEM, North Haugh, St Andrews, Fife, UK

[*]Correspondence to: Department of Bioengineering, Nagaoka University of Technology, Nagaoka, Niigata, Japan

E-mail address: emasai@vos.nagaokaut.ac.jp (E. Masai)

Abstract

Microbial conversions known as “biological funneling” have attracted attention for their ability to upgrade heterogeneous mixtures of low-molecular-weight aromatic compounds obtained by chemical lignin depolymerization. β-hydroxypropiovanillone (HPV) and its analogs can be obtained by chemoselective catalytic oxidation of lignin using 2,3-dichloro-5,6-dicyano-1,4-benzoquinone/*tert*-butyl nitrite/O_2, followed by cleavage of arylglycerol-β-aryl ether with zinc. *Sphingobium* sp. strain SYK-6 can degrade HPV generated by the catabolism of arylglycerol-β-aryl ether through 2-pyrone-4,6-dicarboxylate (PDC), a promising platform chemical. Therefore, production of PDC from HPV can be achieved using the HPV catabolic pathway. However, the pathway and genes involved in the catabolism of vanilloyl acetic acid (VAA) generated during HPV catabolism have not been investigated. In the present study, we isolated SLG_24960 (*vceA*), which encodes an enzyme that converts VAA into a coenzyme A (CoA) derivative of vanillate (vanilloyl-CoA) from SYK-6, by shotgun cloning. The analysis of a *vceA* mutant indicated that this gene is not required for VAA conversion *in vivo*, but it encodes a major enzyme catalyzing CoA-dependent VAA conversion *in vitro*. We also identified SLG_12450 (*vceB*), whose product can convert vanilloyl-CoA to vanillate. Enzyme genes besides *vceA* and *vceB*, which are necessary for the conversions of HPV to VAA and of vanillate to PDC, were introduced and expressed in *Pseudomonas putida*. The resulting engineered strain completely converted 1 mM HPV into PDC after 24 h. Our results suggest that the enzyme genes that are not required for the catabolic pathway in microorganisms but can be used for the conversion of target substrates are buried in microbial genomes. These genes are, thus, useful for designing metabolic pathways to produce value-added metabolites.

Keywords: *Sphingobium* sp. SYK-6; lignin; β-aryl ether; 2-pyrone-4,6-dicarboxylate; β-keto acid cleavage enzyme

1. Introduction

Lignin, a major component of plant cell walls, is a complex phenolic heteropolymer produced from hydroxycinnamyl alcohols by radical coupling (Boerjan et al., 2003; Ralph et al., 2004). Lignin is the second most abundant bioresource on Earth after cellulose, and it can potentially be used as an industrial raw material. However, the effective utilization of lignin has not yet been established, which is mainly due to its structural complexity (Himmel et al., 2007). In recent years, microbial conversions known as "biological funneling" have attracted attention for their ability to upgrade heterogeneous mixtures of low-molecular-weight aromatic compounds obtained by chemical lignin depolymerization into platform chemicals (Beckham et al., 2016; Linger et al., 2014; Masai et al., 2007; Otsuka et al., 2006).

β-aryl ether is the most abundant interunit linkage in lignin, accounting for 45%–50% and 60%–62% of the total linkages in softwood and hardwood lignin, respectively (Zakzeski et al., 2010). Accordingly, degradation of this structure is considered a crucial step in lignin degradation. β-aryl ether-type biaryls have two distinct isomeric forms, *erythro* and *threo*, each of which has enantiomeric forms (Akiyama et al., 2000). *Sphingobium* sp. strain SYK-6 is an alphaproteobacterium with the best-characterized catabolic systems for lignin-derived aromatic compounds (Kamimura et al., 2017; Masai et al., 2007). SYK-6 can utilize various lignin-derived biaryls, including β-aryl ether, phenylcoumaran, biphenyl, and diarylpropane, as well as monoaryls, including ferulate, vanillin, and syringaldehyde, as the sole source of carbon and energy. In SYK-6 cells, four stereoisomers of the model β-aryl ether dimeric compound guaiacylglycerol-β-guaiacyl ether (GGE) are converted into two enantiomers of α-(2-methoxyphenoxy)-β-hydroxypropiovanillone (MPHPV) through the oxidation of the GGE α-carbon atom catalyzed by Cα-dehydrogenases, LigD, LigL, and LigN (Fig. 1) (Sato et al., 2009). LigD oxidizes (α*R*,β*S*)-GGE and (α*R*,β*R*)-GGE into (β*S*)-MPHPV

and (β*R*)-MPHPV, respectively, whereas LigL/LigN converts (α*S*,β*R*)-GGE and (α*S*,β*S*)-GGE into (β*R*)-MPHPV and (β*S*)-MPHPV, respectively. The ether linkage in the resulting MPHPV is cleaved by enantioselective glutathione *S*-transferases (GSTs), LigF, LigE, and LigP (β-etherases), to produce α-glutathionyl-β-hydroxypropiovanillone (GS-HPV) and guaiacol via the nucleophilic attack of the glutathione on the MPHPV β-carbon atom (Fig. 1) (Gall et al., 2014; Masai et al., 2003; Tanamura et al., 2011). LigF and LigE/LigP attack (β*S*)-MPHPV and (β*R*)-MPHPV to produce (β*R*)-GS-HPV and (β*S*)-GS-HPV, respectively (Gall et al., 2014; Hishiyama et al., 2012; Masai et al., 2003; Tanamura et al., 2011). LigG, another GST, catalyzes the cleavage of the thioether linkage in (β*R*)-GS-HPV by transferring the glutathione of (β*R*)-GS-HPV to another glutathione molecule to produce β-hydroxypropiovanillone (HPV) and glutathione disulfide (Fig. 1) (Masai et al., 2003; Meux et al., 2012). A recent study has reported that GST-encoding SLG_04120 exhibits GSH-eliminating activity of both GS-HPV isomers (Kontur et al., 2018).

HPV and β-hydroxypropiosyringone (HPS, an intermediate metabolite of syringyl-type β-aryl ether) are converted into vanilloyl acetaldehyde (VAL) and 3-(4-hydroxy-3,5-dimethoxyphenyl)-3-oxopropanal (SAL), respectively, via oxidation of the alcohol group at the Cγ-position of HPV and HPS by HpvZ, which belong to the glucose-methanol-choline oxidoreductase family (Fig. 1) (Higuchi et al., 2018). VAL and SAL are further converted into vanilloyl acetic acid (VAA) and 3-(4-hydroxy-3,5-dimethoxyphenyl)-3-oxopropanoic acid (SAA), respectively, via oxidation of the aldehyde group at the Cγ-position of VAL and SAL by multiple benzaldehyde dehydrogenases, including SLG_20400 (Fig. 1). In our previous study, we suggested that VAA and SAA are catabolized via vanillate and syringate through activation of VAA and SAA by coenzyme A (CoA) (Higuchi et al., 2018). Although feruloyl-CoA synthetase (FerA) has the ability to convert VAA into its CoA derivative (VAA-CoA),

this gene is not required for VAA conversion (Higuchi et al., 2018). Therefore, the genes primarily responsible for the conversion of VAA and SAA remain unknown.

It has recently been demonstrated that certain biological and chemical treatments of lignin produce HPV and HPS as products. Ohta et al. reported that HPV and HPS were obtained from milled wood lignin after incubation with β-aryl ether cleavage enzymes (SDR3, SDR5, GST3, GST4, and GST5) of *Novosphingobium* sp. MBES04 (Ohta et al., 2017). Similarly, HPV and HPS were obtained from maize corn stover lignin by incubation with LigD, LigN, LigE, and LigF of SYK-6 and Nu class GST of *Novosphingobium aromaticivorans* DSM 12444 under conditions wherein NAD^+ and glutathione were recycled (Gall et al., 2018). Regarding chemical processing, Lancefield et al. reported an isolation method for HPV and HPS from birch lignin via catalytic oxidation of the β-aryl ether linkage in lignin, followed by zinc-mediated cleavage of the ether bonds (Lancefield et al., 2015). In the SYK-6 catabolic pathway of HPV and HPS, 2-pyrone-4,6-dicarboxylate (PDC; a promising platform chemical for functional polyamides, polyesters, and polyurethanes) is generated as an intermediate metabolite (Fig. 1) (Higuchi et al., 2018; Hishida et al., 2009; Masai et al., 1999; Michinobu et al., 2009; Shikinaka et al., 2018). To date, PDC production from protocatechuate (Otsuka et al., 2006), and vanillin, vanillate, and syringaldehyde obtained from kraft lignin, Japanese cedar, and birch (Qian et al., 2016) has been achieved using engineered strains of *Pseudomonas putida* PpY1100. Recently, PDC production has attracted attention; PDC production from lignin-derived or lignin-related aromatic compounds and some lignin depolymerization products using engineered *N. aromaticivorans* DSM 12444 and *P. putida* KT2440 has been reported (Johnson et al., 2019; Perez et al., 2019). A new strategy to utilize lignin can be established by combining chemical or biological processes that produce HPV and HPS with the SYK-6 catabolic system to produce PDC.

In the present study, we identified and functionally characterized two novel SYK-6

genes whose products can convert VAA/SAA into vanilloyl-CoA/syringoyl-CoA and vanilloyl-CoA/syringoyl-CoA into vanillate/syringate. Using these genes as well as other HPV/HPS catabolic genes, we metabolically engineered *P. putida* to produce PDC from HPV.

2. Materials and Methods

2.1. Bacterial strains, plasmids, and culture conditions

The strains and plasmids used in this study are listed in Table S1. *Sphingobium* sp. strain SYK-6 and its mutants were grown in lysogeny broth (LB); Wx minimal medium (Kasai et al., 2012) containing 10 mM sucrose, 10 mM glutamate, 0.13 mM methionine, and 10 mM proline (Wx-SEMP); and Wx-SEMP containing 2 mM GGE or HPV at 30°C. *Sphingobium japonicum* UT26S and *P. putida* PpY1100 were grown in LB at 30°C. When necessary, 50 mg/L kanamycin, 100 mg/L streptomycin, or 12.5 mg/L tetracycline was added to the cultures. *Escherichia coli* strains were grown in LB at 37°C. For cultures of cells carrying antibiotic resistance markers, the media for *E. coli* transformants were supplemented with 100 mg/L ampicillin, 25 mg/L kanamycin, or 12.5 mg/L tetracycline.

2.2. Preparation of substrates

HPV and HPS were prepared as described previously (Higuchi et al., 2018). For the preparation of VAA and SAA, HPV or HPS (final concentration: 1 mM) was added to 20 mL of the cell suspensions of *E. coli* BL21(DE3) cells harboring pCold12830 (final optical density at 600 nm [OD_{600}] of 50.0) and *E. coli* BL21(DE3) cells harboring pT21-2040 (final OD_{600} of 15.0). After incubation with shaking for 12 h at 30°C, the cultures were centrifuged at 19,000 ×*g* for 15 min, and the supernatants were filtered using an Amicon Ultra spin filter unit (3 kDa cutoff; Millipore). The resulting filtrates were used in the preparation of 1 mM VAA and SAA. PDC was prepared as described previously (Otsuka et al., 2006). Other aromatic compounds were purchased from Tokyo Chemical Ind., Co., Ltd.; Sigma-Aldrich Co., LLC.; and FUJIFILM Wako Pure Chemical Corporation.

161

162 *2.3. Conversion of VAA by cell extracts and resting cells*

163 SYK-6 cells grown in LB were inoculated into the same medium (final concentration:
164 1%) and incubated for 24 h. The resultant cells were washed twice with 50 mM Tris-
165 HCl buffer (pH 7.5, Buffer A). Cells resuspended in the same buffer were then broken
166 using an ultrasonic disintegrator (QSonica Q125; WakenBtech Co., Ltd.). After
167 centrifugation at 19,000 ×*g* for 15 min at 4°C, the supernatants were obtained as cell
168 extracts. Protein concentration was determined using the Bradford method with bovine
169 serum albumin as the standard (Bio-Rad Laboratories). The cell extracts (200–1,000 μg
170 protein/mL) of SYK-6 were incubated in Buffer A containing 100 μM VAA in the
171 presence and absence of cofactors (1 mM CoA + 1.25 mM ATP + 1.25 mM $MgSO_4$,
172 1 mM acetyl-CoA, or 1 mM succinyl-CoA) for 5 min at 30°C. The reactions were
173 stopped by the addition of acetonitrile (final concentration: 50%). Precipitated proteins
174 were removed by centrifugation at 19,000 ×*g* for 15 min, and the resulting supernatants
175 were diluted with water (final concentration: 25%), filtered, and analyzed using high-
176 performance liquid chromatography (HPLC). Specific activity was expressed in moles
177 of VAA converted per minute per milligram of protein.

178 For resting-cell assays, SYK-6 cells grown in LB were inoculated into Wx-SEMP
179 to an OD_{600} of 0.2 and grown at 30°C. GGE or HPV (2 mM) was added when the OD_{600}
180 of the culture reached 0.5, and the culture was then further incubated for 6 h. Cells were
181 collected by centrifugation at 5,000 ×*g* for 5 min, washed twice with Buffer A, and
182 resuspended in the same buffer. The resultant cell suspensions were used as resting cells.
183 Resting cells (OD_{600} = 2.0) were mixed with 100 μM VAA and incubated for 8 h at
184 30°C with shaking. Portions of the cultures were periodically collected, and the
185 reactions were stopped by centrifugation. The amount of VAA was measured using
186 HPLC.

187

188

189 *2.4. HPLC–mass spectrometry analysis*

190 HPLC–mass spectrometry (HPLC–MS) analysis was performed with the ACQUITY
191 UPLC system (Waters) coupled with an ACQUITY TQ detector using a TSKgel ODS-
192 140HTP column (2.1 × 100 mm; Tosoh) as described previously (Fukuhara et al.,
193 2010). All analyses were performed at a flow rate of 0.5 mL/min. The mobile phase was
194 a mixture of Solution A (acetonitrile containing 0.1% formate) and Solution B (water
195 containing 0.1% formate) with the following conditions: *detection of the reaction*
196 *products of VAA and syringate generated from SAA*: 0–4.0 min, linear gradient from 5%
197 to 15% A; 4.0–4.2 min, decreasing gradient from 15% to 5% A; 4.2–5.0 min, 5% A.
198 *Detection of the reaction products of SAA and VAA in the presence of propionyl-CoA*:
199 0–5.0 min, linear gradient from 5% to 10% A; 5.0–5.2 min, decreasing gradient from
200 10% to 5% A; 5.2–6.0 min, 5% A. *Detection of the reaction products of VAA in the*
201 *presence of butyryl-CoA*: 0–7.0 min, linear gradient from 2% to 10% A; 7.0–7.2 min,
202 decreasing gradient from 10% to 2% A; 7.2–8.0 min, 2% A. *Detection of the reaction*
203 *products of caffeate*: 0–3.0 min, linear gradient from 5% to 25% A; 3.0–3.2 min,
204 decreasing gradient from 25% to 5% A; 3.2–4.0 min, 5% A. *Detection of the reaction*
205 *products of ferulate, sinapate, p-coumarate, 3-(4-hydroxy-3-methoxyphenyl)propionate,*
206 *homovanillate, vanillylmandelate, and vanillate*: 0–5.0 min, 10% A. *Detection of the*
207 *reaction products of cinnamate*: 0–5.0 min, 25% A. For the analysis of the reaction
208 products of HPV, the mobile phase was a mixture of water (95%) and acetonitrile (5%)
209 containing 0.1% phosphate. VAA, SAA, vanilloyl-CoA, syringoyl-CoA, vanillate,
210 syringate, ferulate, sinapate, *p*-coumarate, cinnamate, caffeate, 3-(4-hydroxy-3-
211 methoxyphenyl)propionate, homovanillate, vanillylmandelate, and PDC were detected
212 at 280, 307, 300, 300, 260, 275, 322, 323, 310, 278, 323, 279, 279, 311, and 315 nm,
213 respectively. In the electrospray ionization–MS (ESI–MS) analysis, MS spectra were
214 obtained using the negative-ion mode with the settings reported in our previous study

(Fukuhara et al., 2010).

2.5. Gene cloning

A partially SalI-digested gene library of SYK-6 constructed with pVK100 in *E. coli* was introduced into the host strain *S. japonicum* UT26S by triparental mating (Ditta et al., 1980). The ability of 330 transconjugants grown in diluted LB to transform 50 μM VAA was analyzed by HPLC. SalI fragments of pVA17 and pVA116 isolated from the transconjugants (No. 17 and No. 116, respectively) were cloned into pBluescript II KS(+). The nucleotide sequences of both ends of the inserts were determined, and the complete sequences were retrieved from the genome sequence of SYK-6 (accession number: AP012222). To examine whether each of the seven cosmids contained SLG_24820 or its homolog, polymerase chain reaction (PCR) was performed using the seven cosmids as templates and the primer pairs listed in Table S2.

2.6. Analysis of nucleotide and amino acid sequences

Nucleotide sequences were determined by Eurofins Genomics. Sequence analysis was performed using the MacVector program (MacVector, Inc.). Sequence similarity searches, pairwise alignments, and multiple alignments were conducted using the BLASTP program (Johnson et al., 2008), the EMBOSS Needle program through the EMBL-EBI server (Li et al., 2015), and the Clustal Omega program (Sievers et al., 2011), respectively.

2.7. Expression of SLG_24820, vceA, and vceB in E. coli and enzyme purification

DNA fragments carrying SLG_24820, SLG_24960 (*vceA*), and SLG_12450 (*vceB*) were amplified by PCR using SYK-6 total DNA and the primer pairs listed in Table S2. Amplified fragments carrying SLG_24820, *vceA*, and *vceB* were cloned into pET-16b to obtain pET24820, pET24960, pET12450, respectively. Nucleotide sequences of their

242 inserts were confirmed by sequencing. To generate pCold24820, the 0.9 kb NdeI-
243 BamHI fragment of pET24820 was inserted into pCold I. The expression plasmids were
244 introduced into *E. coli* BL21(DE3), and the transformed cells were grown in LB.
245 Expression of SLG_24820 and other genes was induced for 24 h at 16°C and 4 h at
246 30°C, respectively, by adding 1 mM isopropyl-β-D-thiogalactopyranoside when the
247 OD_{600} of the cultures reached 0.5. Cells were then harvested by centrifugation at
248 5,000 ×*g* for 5 min at 4°C and washed with Buffer A. The resultant cultures were
249 washed twice with Buffer A, and the cells were then resuspended in the same buffer and
250 broken by an ultrasonic disintegrator. After centrifugation at 19,000 ×*g* for 15 min at
251 4°C, the supernatants were obtained as cell extracts. For purification of VceA, a cell
252 extract of *E. coli* BL21(DE3) harboring pET24960 was applied to a His SpinTrap
253 column (GE Healthcare). Purified fractions were subjected to desalting and
254 concentrating using an Amicon Ultra spin filter unit (30 kDa cutoff; Merck Millipore),
255 and the enzyme preparation was stored at −80°C. The expression of genes and the
256 purity of preparations were examined using sodium dodecyl sulfate (SDS)–12%
257 polyacrylamide gel electrophoresis (PAGE). Protein bands in gels were stained with
258 Coomassie Brilliant Blue.
259
260 *2.8. Identification of reaction products*
261 In the presence of 0.2–1.0 mM acetyl-CoA, VAA or SAA (100 μM) was incubated with
262 the cell extract of *E. coli* BL21(DE3) harboring pET24820 (800 μg protein/mL), cell
263 extract of *E. coli* BL21(DE3) harboring pET24960 (100 μg protein/mL), or purified
264 VceA (10 μg protein/mL) for 10–120 min at 30°C. The reaction mixtures were then
265 analyzed using HPLC–MS under the conditions described above.
266
267 *2.9. Construction of mutants*
268 To construct the mutants of SLG_24820, *vceA*, and *vceB*, the upstream and downstream

regions (ca. 1.0 kb each) of the genes were amplified by PCR from SYK-6 total DNA using the primer pairs listed in Table S2. The resulting fragments were cloned into pAK405 (Kaczmarczyk et al., 2012) by In-Fusion Cloning (Takara Bio). Each of the resulting plasmids was introduced into SYK-6 cells by triparental mating, and the resulting mutants were selected as described previously (Kaczmarczyk et al., 2012). Gene deletion was confirmed by colony PCR using the primer pairs listed in Table S2. For complementation of the *vceA* mutant (Δ2496), pQF24960 was introduced into Δ2496 cells by electroporation. The transformed cells were then grown in LB containing 100 μM cumate and tetracycline for 24 h.

2.10. Characterization of Δ2482 and Δ2496

SYK-6, SLG_24820 mutant (Δ2482), and Δ2496 cells were grown in LB. After 24 h of incubation, cells were collected by centrifugation, washed twice with Buffer A, and resuspended in the same buffer. After the addition of 100 μM VAA or SAA, resting cells (OD_{600} of 0.5) were incubated at 30°C with shaking for 8 h. Portions of the cultures were periodically collected, and the amounts of the substrates were measured using HPLC. Cell extracts (2–1,000 μg protein/mL) of SYK-6, Δ2482, Δ2496, and their complemented strains were incubated with 100 μM VAA in the presence of cofactors in Buffer A for 5 min at 30°C. The supernatants of the reaction mixtures were analyzed using HPLC.

2.11. Analysis of enzyme properties

The enzyme reaction was conducted by incubating purified VceA (1–50 μg protein/mL) with 100 μM VAA, 100 μM $CoSO_4 \cdot 7H_2O$, and 1 mM acetyl-CoA in Buffer A for 3 min at 30°C. After incubation, the amounts of VAA were measured using HPLC. To examine metal ion dependency, 500 μM ethylenediaminetetraacetic acid (EDTA) was added to Buffer A containing purified VceA (5 μg protein/mL). After incubation for

20 h on ice, EDTA-treated VceA was incubated with 100 μM VAA and 1 mM acetyl-CoA for 3 min at 30°C. To examine the effect of metal ions on enzyme activity, VceA (1–5 μg protein/mL) was incubated with 100 μM VAA and 1 mM acetyl-CoA in the presence and absence of 100 μM $ZnCl_2$, $FeCl_2 \cdot 4H_2O$, $MgCl_2 \cdot 6H_2O$, $MnCl_2 \cdot 4H_2O$, $CaCl_2 \cdot 2H_2O$, $CuSO_4 \cdot 5H_2O$, $CoSO_4 \cdot 7H_2O$, and $Na_2MoO_4 \cdot 2H_2O$ for 3 min at 30°C. To examine CoA donor specificity, VceA (1–50 μg protein/mL) was incubated with 100 μM VAA and 100 μM $CoSO_4 \cdot 7H_2O$ in the presence and absence of 1 mM CoA, acetyl-CoA, propionyl-CoA, butyryl-CoA, malonyl-CoA, acetoacetyl-CoA, succinyl-CoA, and benzoyl-CoA. The optimum pH was determined from a pH range from 5.0 to 9.0 using 50 mM GTA buffer (50 mM 3,3-dimethylglutaric acid, 50 mM Tris, and 50 mM 2-amino-2-methyl-1,3-propanediol) at 30°C. The optimum temperature was determined from a temperature range from 10°C to 70°C using Buffer A. To determine the substrate range, 100 μM VAA, SAA, ferulate, sinapate, *p*-coumarate, cinnamate, caffeate, 3-(4-hydroxy-3-methoxyphenyl)propionate, homovanillate, vanillylmandelate, and vanillate were used for the reaction, and the conversion of substrates and generation of reaction products were analyzed using HPLC–MS.

2.12. Enzyme activity of VceB

Crude VceB was prepared from *E. coli* harboring pET12450 as described above. Purified VceA (1 μg protein/mL) and crude VceB (5 μg protein/mL) were incubated with 100 μM VAA or SAA, 100 μM $CoSO_4 \cdot 7H_2O$, and 1 mM acetyl-CoA in Buffer A for 30 min at 30°C. The reaction mixtures were analyzed using HPLC. Purified VceA (10 μg protein/mL) and cell extract of SYK-6 or Δ1245 (20 μg protein/mL) were incubated with 100 μM VAA or SAA, 100 μM $CoSO_4 \cdot 7H_2O$, and 1 mM acetyl-CoA in Buffer A for 60 min at 30°C. Portions of the reaction mixtures were collected at various sampling time points and analyzed using HPLC.

2.13. PDC production from HPV

Each gene fragment carrying *hpvZ*, SLG_20400, *vceA*, and *vceB* was amplified by PCR using SYK-6 total DNA and the primer pairs listed in Table S2. Upstream sequences containing a ribosome-binding site of each gene were designed using the RBS calculator ver. 2.0 (https://salislab.net/software/forward) (Salis et al., 2009) to maximize the translation rate and were included in the primer sequences. The resulting fragments were cloned into the BamHI site of pJB866 by In-Fusion Cloning to generate pJHV01. pJHV01 or pJB866 was introduced into *P. putida* PpY1100 cells harboring pDVZ21 [PpY1100(pDVZ21)] by electroporation or triparental mating. Cells of PpY1100(pJB866-pDVZ21) and PpY1100(pJHV01-pDVZ21) were then grown in LB containing kanamycin and tetracycline for 12 h. The cells were harvested by centrifugation at 5,000 ×*g* for 5 min, washed twice with Wx medium, and resuspended in 5 mL of the same medium. The cells were then inoculated into 5 mL of Wx medium containing 20 mM glucose, 1 mM, 2 mM, or 5 mM HPV, 1 mM *m*-toluate, kanamycin, and tetracycline to an OD_{600} of 0.2 and incubated with shaking for 30 h at 30°C. Cell growth was measured by OD_{600}. Portions of the cultures were periodically collected, and the reactions were stopped by centrifugation. The resultant supernatants were diluted, filtered, and analyzed using HPLC.

3. Results and Discussion

3.1. Detection of VAA-converting enzyme activity in Sphingobium sp. SYK-6

In a previous study, our findings suggested that VAA was converted into vanillate through activation of VAA by CoA in SYK-6 (Higuchi et al., 2018). To characterize the enzymes involved in the catabolism of VAA in SYK-6, the cofactor requirements and induction profiles of VAA-converting activities in SYK-6 were examined. The extract of SYK-6 cells grown in LB was incubated with 100 μM VAA in the presence of 1 mM CoA + 1.25 mM ATP + 1.25 mM $MgSO_4$, 1 mM acetyl-CoA, or 1 mM succinyl-CoA. HPLC analyses of the reaction mixtures indicated that VAA was converted into vanillate in the presence of each cofactor but not without the cofactors (Fig. 2A). The specific activity in the presence of acetyl-CoA (35 ± 3 $nmol \cdot min^{-1} \cdot mg^{-1}$) was 4.1- and 11-fold higher than those obtained in the presence of CoA + ATP + Mg^{2+} and succinyl-CoA, respectively (Fig. 2A). These results suggest the involvement of a CoA-dependent enzyme, in particular an acetyl-CoA-dependent enzyme, in VAA catabolism.

To examine the inducibility of the VAA-converting enzyme in SYK-6, resting cells of SYK-6 grown in Wx-SEMP, Wx-SEMP + GGE, or Wx-SEMP + HPV were incubated with 100 μM VAA for 6 h. The conversion rates of cells grown with and without GGE were almost identical, although the rate of cells grown with HPV was slightly lower than that of cells grown without HPV (Fig. S1). Therefore, it appears that the gene(s) responsible for the conversion of VAA are not induced during GGE degradation.

3.2. Isolation of genes involved in the conversion of VAA

A cosmid library of SYK-6 constructed in *S. japonicum* UT26S was screened for clones capable of converting VAA. Among the 330 clones tested, seven transconjugants converted VAA into vanillate at 48 h (Fig. S2). The generation of vanillate suggests that

368 VAA was subjected to Cα-Cβ cleavage. Two cosmid clones, pVA17 and pVA116,
369 were isolated from the transconjugants (No. 17 and No. 116), and the nucleotide
370 sequences of the SalI fragments of pVA17 and pVA116 were determined. This analysis
371 showed that both clones contained SLG_24820, which exhibits 31% amino acid
372 sequence identity with the 3-keto-5-aminohexanoate cleavage enzyme (Kce) from
373 *Candidatus Cloacamonas acidaminovorans* (Bellinzoni et al., 2011). Kce is known to
374 catalyze the reversible condensation reaction between 3-keto-5-aminohexanoate and
375 acetyl-CoA to form 3-aminobutyryl-CoA and acetoacetate in the lysine fermentation
376 pathway of *Clostridium* SB4, *Brevibacterium* sp. L5, and *Fusobacterium nucleatum*
377 (Fig. S3A) (Barker et al., 1980; Barker et al., 1982; Bellinzoni et al., 2011; Kreimeyer et
378 al., 2007; Yorifuji et al., 1977). A BLAST search of the SYK-6 genome database
379 revealed the presence of three genes (SLG_12200, SLG_12450, and SLG_24960), thus
380 showing 26%–28% amino acid sequence identity with SLG_24820. To clarify whether
381 each cosmid contains SLG_24820 or its homolog, PCR was performed using primers
382 specifically amplifying the abovementioned four genes. The results showed that
383 SLG_24820 was amplified when pVA17 and pVA116 were used as templates, whereas
384 SLG_24960 was amplified from other cosmids (data not shown). These results suggest
385 the involvement of SLG_24820 and/or SLG_24960 in the conversion of VAA.
386
387 *3.3. Gene products of SLG_24820 and SLG_24960 catalyze Cα-Cβ cleavage of VAA*
388 To examine whether the gene products of SLG_24820 and SLG_24960 have the ability
389 to convert VAA, SLG_24820 and SLG_24960 fused with a His tag at the 5′ terminus
390 were expressed in *E. coli*. SDS-PAGE showed the production of a 34-kDa protein in
391 each cell extract of *E. coli*(pET24820) and *E. coli*(pET24960) (Fig. S4). Cell extracts of
392 these *E. coli* transformants were incubated with 100 μM VAA in the presence of 1 mM
393 acetyl-CoA to identify the reaction products. HPLC–MS analysis showed that the cell
394 extract of *E. coli*(pET24960) converted VAA into vanillate (retention time: 2.4 min)

and Compound I (3.1 min) after 10 min of incubation (Fig. 3A and B). Negative ESI–MS analysis of Compound I showed fragments at *m*/*z* 916 ($[M - H]^-$) and 458 ($[M - 2H]^{2-}$). Based on the molecular weight deduced from the fragment ions, Compound I was identified as vanilloyl-CoA (MW: 917.67) (Fig. 3C and F). Conversely, the cell extract of *E. coli*(pET24820) converted VAA into vanillate after 2 h of incubation (Fig. 3D and E). These results suggest that SLG_24960 and SLG_24820 catalyze the Cα-Cβ cleavage of VAA with the addition of CoA. The resulting vanilloyl-CoA appears to have been converted into vanillate by enzyme activity derived from the host strain.

3.4. Disruption of SLG_24820 and SLG_24960 in SYK-6

To examine whether SLG_24820 and SLG_24960 are indeed involved in the conversion of VAA and SAA in SYK-6, SLG_24820 (Δ2482) and SLG_24960 (Δ2496) mutants were created (Fig. S5). The ability of Δ2482 and Δ2496 to convert 100 μM VAA and SAA was assessed using resting cells. The results showed that both mutant cells converted VAA and SAA comparably to the wild type (Fig. S6). Subsequently, cell extracts of both mutants were incubated with 100 μM VAA and SAA, respectively, in the presence of 1 mM CoA + 1.25 mM ATP + 1.25 mM $MgSO_4$, 1 mM acetyl-CoA, or 1 mM succinyl-CoA. The Δ2482 cell extract showed activity toward VAA and SAA comparable to that of the wild type in the presence of each cofactor (Fig. 2A and B). Conversely, the VAA conversion activity by the Δ2496 cell extract was significantly decreased in the presence of CoA + ATP + Mg^{2+} (44% of the activity of the wild type) and acetyl-CoA (22% of the activity of the wild type) and was almost lost with succinyl-CoA (Fig. 2A). When SAA was used as a substrate, no conversion was observed in the presence of any cofactor (Fig. 2B). To determine whether this activity defect was due to the disruption of SLG_24960, pQF carrying SLG_24960 (pQF24960) was introduced into Δ2496 cells. The VAA conversion activity of the cell extract of Δ2496(pQF24960) increased 6- and 113-fold over the vector-control strain in the

presence of CoA + ATP + Mg^{2+} and acetyl-CoA, respectively, and the activity was also observed in the presence of succinyl-CoA (Fig. 2C). Given these results, it was concluded that SLG_24960 and SLG_24820 are not required for VAA and SAA catabolism in SYK-6. In addition, the cell extract of Δ2496 showed no activity toward SAA even in the presence of acetyl-CoA, although its activity toward VAA remained. This suggests that another CoA-dependent enzyme with low activity but high specificity for VAA is present in SYK-6.

Here we found that SYK-6 has an extra VAA-converting enzyme gene (SLG_24960), which may be useful for designing a VAA conversion pathway. Considering that the gene product of SLG_24960 may convert VAA into vanilloyl-CoA, it may be possible to convert VAA into vanillate by expressing the vanilloyl-CoA thioesterase gene in addition to SLG_24960. Furthermore, a microbial cell factory that converts HPV obtained from lignin into PDC can be established if SLG_24960 and the vanilloyl-CoA thioesterase gene are coexpressed in a host microbe with the enzyme genes necessary for the conversion of HPV into VAA and of vanillate into PDC. Therefore, we designated SLG_24960 as *vceA* and investigated the enzymatic properties of the gene product.

3.5. Identification of the reaction product of VceA

VceA was purified to near homogeneity by Ni affinity chromatography from the cell extract of *E. coli* expressing His-tagged *vceA* (Fig. S4). Purified VceA was incubated with 100 μM VAA in the presence of 200 μM acetyl-CoA for 30 min. HPLC analysis of the reaction mixture showed that VceA converted VAA into vanilloyl-CoA without generating vanillate (Fig. S7B). Similarly, VceA converted SAA into syringoyl-CoA (Fig. S7D–F). Thus, VceA was confirmed to catalyze the conversion of VAA and SAA into vanilloyl-CoA and syringoyl-CoA, respectively. Three-dimensional structure analysis of Kce from *Candidatus Cloacamonas acidaminovorans* indicated that His46,

His48, and Glu230 are responsible for the coordination of the metal ion and that the Asp231–Arg226 charge-relay dyad is involved in the abstraction of the pro-*S* proton from C2 of 3-keto-5-aminohexanoate (Fig. S3B) (Bellinzoni et al., 2011). Kce catalyzes the condensation reaction between 3-keto-5-aminohexanoate and acetyl-CoA by a Zn^{2+}-dependent Claisen-like mechanism to generate 3-aminobutyryl-CoA and acetoacetate (Heath and Rock, 2002). All these residues are conserved in VceA (Fig. S8), which is likely to convert VAA and SAA by a mechanism similar to that for Kce.

3.6. Enzyme properties of VceA

To examine the metal ion dependency of VceA, VceA was treated with 500 μM EDTA. The specific activity of EDTA-treated VceA was reduced to approximately 50% (0.9 ± 0.2 $\mu mol \cdot min^{-1} \cdot mg^{-1}$) of the specific activity of untreated enzyme (2.0 ± 0.1 $\mu mol \cdot min^{-1} \cdot mg^{-1}$). The effects of metal ions [Zn^{2+}, Fe^{2+}, Mg^{2+}, Mn^{2+}, Ca^{2+}, Cu^{2+}, Co^{2+}, and Mo^{2+} (100 μM)] on enzyme activity were evaluated. The specific activities of VceA in the presence of Mn^{2+} and Co^{2+} were 4.8- and 8.7-fold higher than that of the control, respectively; however, the addition of other metal ions, including Zn^{2+}, which is the important metal ion for Kce, had no effect on enzyme activity (Table S3). These results suggest that VceA requires Co^{2+} or Mn^{2+} for its activity, which differs from Kce that requires Zn^{2+}.

To examine the CoA donor specificity of VceA, VceA was incubated with VAA in the presence of 1 mM CoA, acetyl-CoA, propionyl-CoA, butyryl-CoA, malonyl-CoA, acetoacetyl-CoA, succinyl-CoA, and benzoyl-CoA (Table S4). The highest activity (100%) was obtained in the presence of acetyl-CoA, whereas 33% activity was observed with propionyl-CoA. The activity was less than 1% in the presence of the other CoA donor. These results indicate that VceA is highly specific to acetyl-CoA. Vanilloyl-CoA was produced in each reaction regardless of the CoA donor. When using cell extracts of SYK-6, VAA conversions were observed in the presence of CoA + ATP

476 + Mg^{2+} and succinyl-CoA (Fig. 2A), although VceA is unable to utilize these cofactors.
477 The SYK-6 enzyme activities for VAA in the presence of CoA and succinyl-CoA
478 appear to be the sum of activities of the abovementioned unidentified CoA-dependent
479 enzyme and VceA. In SYK-6 cell extracts, endogenous enzymes may produce a certain
480 amount of acetyl-CoA that is necessary for VceA using CoA and succinyl-CoA.
481 The optimum pH and temperature for VceA activity were determined to be 7.5–8.0
482 and 50°C, respectively (Fig. S9). The substrate range of VceA was examined using
483 100 μM VAA, SAA, ferulate, sinapate, *p*-coumarate, cinnamate, caffeate, 3-(4-hydroxy-
484 3-methoxyphenyl)propionate, homovanillate, vanillylmandelate, and vanillate (Fig.
485 S10). VceA showed activity only toward VAA (17.4 ± 3.8 $\mu mol \cdot min^{-1} \cdot mg^{-1}$) and SAA
486 (7.6 ± 0.2 $\mu mol \cdot min^{-1} \cdot mg^{-1}$). These results suggest that C6-C3 α-keto acids are
487 substrates for VceA. VceA comprises a DUF849 domain, which is conserved in Kce.
488 Bastard et al. examined the enzyme activity of 124 DUF849-containing proteins
489 extracted from genomic and protein databases toward 17 β-keto acid substrates (Bastard
490 et al., 2014). Although an analog of VAA (4-hydroxy-benzoylacetate) was included in
491 the substrates, none of the proteins showed substantial activity toward this substrate.
492
493 *3.7. Identification of the vanilloyl-CoA/syringoyl-CoA thioesterase gene in SYK-6*
494 The vanilloyl-CoA/syringoyl-CoA thioesterase gene is necessary for the conversion of
495 vanilloyl-CoA/syringoyl-CoA into vanillate/syringate. However, to the best of our
496 knowledge, there is no report on this gene. Conversely, 4-hydroxybenzoyl-CoA
497 thioesterases of the *Pseudomonas* sp. strain CBS3 (C42560) and *Arthrobacter* sp. strain
498 SU (FcbC) have been reported (Chang et al., 1992; Scholten et al., 1991; Song et al.,
499 2012; Song et al., 2007; Zhuang et al., 2003). Because SYK-6 can convert vanilloyl-
500 CoA and syringoyl-CoA (data not shown), we hypothesized that this strain has enzyme
501 genes similar to C42560 or *fcbC*. BLAST searches of the SYK-6 genome database
502 revealed the presence of SLG_12450, which shows 29% amino acid sequence identity

503 with C42560, although no *fcbC* homolog was present. Therefore, SLG_12450 fused
504 with a His tag at the 5′ terminus was expressed in *E. coli*. SDS-PAGE showed the
505 production of a 19-kDa protein in *E. coli* cells harboring pET12450 (Fig. S11).
506 Incubation of 100 μM VAA with VceA and a cell extract of *E. coli* harboring a vector
507 (pET-16b) in the presence of 1 mM acetyl-CoA for 30 min generated vanilloyl-CoA
508 (Fig. 4A and B). Conversely, when VAA was incubated with VceA and a cell extract of
509 *E. coli*(pET12450), VAA was completely converted into vanillate (Fig. 4C). When
510 SAA was used as a substrate, SAA was also completely converted into syringate (Fig.
511 4D–F). These results indicate that SLG_12450 encodes vanilloyl-CoA/syringoyl-CoA
512 thioesterase, and therefore, we designated this gene as *vceB*.
513 To examine whether *vceB* is involved in the conversion of vanilloyl-CoA and
514 syringoyl-CoA in SYK-6, a *vceB* mutant (Δ1245) was created (Fig. S5). When 100 μM
515 VAA or SAA was incubated with VceA and an SYK-6 cell extract in the presence of
516 1 mM acetyl-CoA for 60 min, the substrates were almost completely converted into
517 vanillate and syringate, respectively (Fig. S12). However, only a small amount of
518 vanillate or syringate was generated after 60 min when VAA or SAA was incubated
519 with VceA and a Δ1245 cell extract, indicating that *vceB* is the major gene responsible
520 for the conversion of vanilloyl-CoA and syringoyl-CoA in SYK-6.
521
522 *3.8. PDC production from HPV by engineered P. putida*
523 In our previous study, we demonstrated PDC production from vanillate and syringate
524 using *P. putida* PpY1100 cells harboring pDVZ21, which comprises the vanillate *O*-
525 demethylase gene (*vanAB*) of *P. putida* PpY101, the protocatechuate 4,5-dioxygenase
526 gene (*ligAB*) of SYK-6, and the 4-carboxy-2-hydroxymuconate-6-semialdehyde
527 dehydrogenase gene (*ligC*) of SYK-6 in pKT230MC (Otsuka et al., 2006; Qian et al.,
528 2016). In the present study, we constructed pJHV01, which carries the HPV/HPS
529 oxidase gene (*hpvZ*), the VAL dehydrogenase gene (SLG_20400), *vceA*, and *vceB*

under the control of the same P_m promoter in pJB866 (Fig. 5A). PDC production from HPV using PpY1100 cells harboring pDVZ21 plus pJHV01 was then evaluated. When PpY1100 cells harboring pDVZ21 plus pJB866 (vector) were grown in 20 mM glucose in the presence of 1 mM HPV, no conversion of HPV occurred even after 30 h (Fig. 5B). Conversely, PpY1100(pJHV01-pDVZ21) cells completely converted HPV into PDC after 24 h (Fig. 5C). These results demonstrate that *vceA* and *vceB* are useful for the production of value-added intermediate metabolites, such as PDC from HPV via vanillate (Fig. 1). However, when 2 mM HPV was converted by PpY1100(pJHV01-pDVZ21) cells, approximately 0.3 mM vanillate was accumulated after 72 h, although ca.1.4 mM PDC (70% yield) was obtained. In addition, no HPV conversion was observed when using 5 mM HPV. Therefore, fermentation engineering, including fed-batch, continuous, and high-cell-density cultures, is necessary to improve PDC productivity.

4. Conclusions

To establish microbial conversion of HPV into PDC, we identified and characterized the novel SYK-6 genes *vceA* and *vceB*, which encode an acetyl-CoA-dependent VAA/SAA-converting enzyme and a vanilloyl-CoA/syringoyl-CoA thioesterase, respectively. Using these genes in combination with previously identified genes for converting HPV into VAA (Higuchi et al., 2018) and genes utilized for the production of PDC from vanillate (Otsuka et al., 2006; Qian et al., 2016), we successfully achieved the microbial conversion of HPV derived from guaiacyl lignin into PDC. The HPV conversion system developed here is likely to be applicable in PDC production from HPS derived from syringyl lignin (Fig. 1) (Qian et al., 2016). Given that HPV and HPS can be specifically obtained from lignin by a chemical lignin depolymerization method developed by Lancefield et al.,

557 combining this method with the microbial conversion established here will enable PDC
558 production from lignin (Lancefield et al., 2015). Nevertheless, the total yield of HPV and
559 HPS from the poplar ammonia lignin was only 5.3% (Lancefield et al., 2016); therefore it
560 is necessary to improve HPV and HPS yields and establish a recycling method of organic
561 solvent and a catalyst in future. In addition, our results suggest that enzyme genes that are
562 not required for the catabolic pathway in microorganisms but can be used for the
563 conversion of target substrates are buried in microbial genomes. These genes appear to
564 have applications in the design of metabolic pathways to produce value-added
565 metabolites, and this approach will expand the variation of microbial conversion. We are
566 currently identifying the genes that play a major role in the catabolism of VAA and SAA.

Funding

This research did not receive any specific grant from funding agencies in the public, commercial, or not-for-profit sectors.

References

Akiyama, T., Magara, K., Matsumoto, Y., Meshitsuka, G., Ishizu, A., Lundquist, K., 2000. Proof of the presence of racemic forms of arylglycerol-β-aryl ether structure in lignin: studies on the stereo structure of lignin by ozonation. J. Wood Sci. 46, 414-415.

Barker, H.A., Kahn, J.M., Chew, S., 1980. Enzymes involved in 3,5-diaminohexanoate degradation by *Brevibacterium* sp. J. Bacteriol. 143, 1165-1170.

Barker, H.A., Kahn, J.M., Hedrick, L., 1982. Pathway of lysine degradation in *Fusobacterium nucleatum*. J. Bacteriol. 152, 201-207.

Bastard, K., Smith, A.A., Vergne-Vaxelaire, C., Perret, A., Zaparucha, A., De Melo-Minardi, R., Mariage, A., Boutard, M., Debard, A., Lechaplais, C., Pelle, C., Pellouin, V., Perchat, N., Petit, J.L., Kreimeyer, A., Medigue, C., Weissenbach, J., Artiguenave, F., De Berardinis, V., Vallenet, D., Salanoubat, M., 2014. Revealing the hidden functional diversity of an enzyme family. Nat. Chem. Biol. 10, 42-49.

Beckham, G.T., Johnson, C.W., Karp, E.M., Salvachúa, D., Vardon, D.R., 2016. Opportunities and challenges in biological lignin valorization. Curr. Opin. Biotechnol. 42, 40-53.

Bellinzoni, M., Bastard, K., Perret, A., Zaparucha, A., Perchat, N., Vergne, C., Wagner, T., de Melo-Minardi, R.C., Artiguenave, F., Cohen, G.N., Weissenbach, J., Salanoubat, M., Alzari, P.M., 2011. 3-Keto-5-aminohexanoate cleavage enzyme: a common fold for an uncommon Claisen-type condensation. J. Biol. Chem. 286, 27399-27405.

Boerjan, W., Ralph, J., Baucher, M., 2003. Lignin biosynthesis. Annu. Rev. Plant Biol. 54, 519-546.

Chang, K.H., Liang, P.H., Beck, W., Scholten, J.D., Dunaway-Mariano, D., 1992. Isolation and characterization of the three polypeptide components of 4-chlorobenzoate dehalogenase from *Pseudomonas* sp. strain CBS-3. Biochemistry. 31, 5605-5610.

Ditta, G., Stanfield, S., Corbin, D., Helinski, D.R., 1980. Broad host range DNA cloning system for gram-negative bacteria: construction of a gene bank of

603 *Rhizobium meliloti*. Proc. Natl. Acad. Sci. U. S. A. 77, 7347-7351.
604 Fukuhara, Y., Inakazu, K., Kodama, N., Kamimura, N., Kasai, D., Katayama, Y.,
605 Fukuda, M., Masai, E., 2010. Characterization of the isophthalate degradation
606 genes of *Comamonas* sp. strain E6. Appl. Environ. Microbiol. 76, 519-527.
607 Gall, D.L., Kim, H., Lu, F., Donohue, T.J., Noguera, D.R., Ralph, J., 2014.
608 Stereochemical features of glutathione-dependent enzymes in the *Sphingobium*
609 sp. strain SYK-6 β-aryl etherase pathway. J. Biol. Chem. 289, 8656-8667.
610 Gall, D.L., Kontur, W.S., Lan, W., Kim, H., Li, Y., Ralph, J., Donohue, T.J., Noguera,
611 D.R., 2018. *In vitro* enzymatic depolymerization of lignin with release of
612 syringyl, guaiacyl, and tricin units. Appl. Environ. Microbiol. 84, e02076-17.
613 Heath, R.J., Rock, C.O., 2002. The Claisen condensation in biology. Nat. Prod. Rep. 19,
614 581-596.
615 Higuchi, Y., Aoki, S., Takenami, H., Kamimura, N., Takahashi, K., Hishiyama, S.,
616 Lancefield, C.S., Ojo, O.S., Katayama, Y., Westwood, N.J., Masai, E., 2018.
617 Bacterial catabolism of β-hydroxypropiovanillone and β-
618 hydroxypropiosyringone produced in the reductive cleavage of arylglycerol-β-
619 aryl ether in lignin. Appl. Environ. Microbiol. 84, e02670-17.
620 Himmel, M.E., Ding, S.Y., Johnson, D.K., Adney, W.S., Nimlos, M.R., Brady, J.W.,
621 Foust, T.D., 2007. Biomass recalcitrance: engineering plants and enzymes for
622 biofuels production. Science. 315, 804-807.
623 Hishida, M., Shikinaka, K., Katayama, Y., Kajita, S., Masai, E., Nakamura, M., Otsuka,
624 Y., Ohara, S., Shigehara, K., 2009. Polyesters of 2-pyrone-4,6-dicarboxylic acid
625 (PDC) as bio-based plastics exhibiting strong adhering properties. Polym. J. 41,
626 297-302.
627 Hishiyama, S., Otsuka, Y., Nakamura, M., Ohara, S., Kajita, S., Masai, E., Katayama,
628 Y., 2012. Convenient synthesis of chiral lignin model compounds via optical
629 resolution: four stereoisomers of guaiacylglycerol-β-guaiacyl ether and both
630 enantiomers of 3-hydroxy-1-(4-hydroxy-3-methoxyphenyl)-2-(2-
631 methoxyphenoxy)-propan-1-one (erone). Tetrahedron Lett. 53, 842-845.
632 Johnson, C.W., Salvachúa, D., Rorrer, N.A., Black, B.A., Vardon, D.R., John, P.C.S.,
633 Cleveland, N.S., Dominick, G., Elmore, J.R., Grundl, N., Khanna, P., Martinez,
634 C.R., Michener, W.E., Peterson, D.J., Ramirez, K.J., Singh, P., VanderWall,
635 T.A., Wilson, A.N., Yi, X., Biddy, M.J., Bomble, Y.J., Guss, A.M., Beckham,

636 G.T., 2019. Innovative chemicals and materials from bacterial aromatic
637 catabolic pathways. Joule. 3, 1523-1537.
638 Johnson, M., Zaretskaya, I., Raytselis, Y., Merezhuk, Y., McGinnis, S., Madden, T.L.,
639 2008. NCBI BLAST: a better web interface. Nucleic Acids Res. 36, W5-W9.
640 Kaczmarczyk, A., Vorholt, J.A., Francez-Charlot, A., 2012. Markerless gene deletion
641 system for Sphingomonads. Appl. Environ. Microbiol. 78, 3774-3777.
642 Kamimura, N., Goto, T., Takahashi, K., Kasai, D., Otsuka, Y., Nakamura, M.,
643 Katayama, Y., Fukuda, M., Masai, E., 2017. A bacterial aromatic aldehyde
644 dehydrogenase critical for the efficient catabolism of syringaldehyde. Sci. Rep.
645 7, 44422.
646 Kasai, D., Kamimura, N., Tani, K., Umeda, S., Abe, T., Fukuda, M., Masai, E., 2012.
647 Characterization of FerC, a MarR-type transcriptional regulator, involved in
648 transcriptional regulation of the ferulate catabolic operon in *Sphingobium* sp.
649 strain SYK-6. FEMS Microbiol. Lett. 332, 68-75.
650 Kontur, W.S., Bingman, C.A., Olmsted, C.N., Wassarman, D.R., Ulbrich, A., Gall,
651 D.L., Smith, R.W., Yusko, L.M., Fox, B.G., Noguera, D.R., Coon, J.J.,
652 Donohue, T.J., 2018. *Novosphingobium aromaticivorans* uses a Nu-class
653 glutathione *S*-transferase as a glutathione lyase in breaking the β-aryl ether bond
654 of lignin. J. Biol. Chem. 293, 4955-4968.
655 Kreimeyer, A., Perret, A., Lechaplais, C., Vallenet, D., Médigue, C., Salanoubat, M.,
656 Weissenbach, J., 2007. Identification of the last unknown genes in the
657 fermentation pathway of lysine. J. Biol. Chem. 282, 7191-7197.
658 Lancefield, C.S., Ojo, O.S., Tran, F., Westwood, N.J., 2015. Isolation of functionalized
659 phenolic monomers through selective oxidation and C-O bond cleavage of the β-
660 O-4 linkages in lignin. Angew. Chem. Int. Ed. Engl. 54, 258-262.
661 Lancefield, C.S., Rashid, G.M.M., Bouxin, F., Wasak, A., Tu, W.C., Hallett, J., Zein,
662 S., Rodríguez, J., Jackson, S.D., Westwood, N.J., Bugg, T.D.H., 2016.
663 Investigation of the chemocatalytic and biocatalytic valorization of a range of
664 different lignin preparations: the importance of β-O-4 content. ACS Sustainable
665 Chem. Eng. 4, 6921-6930.
666 Li, W., Cowley, A., Uludag, M., Gur, T., McWilliam, H., Squizzato, S., Park, Y.M.,
667 Buso, N., Lopez, R., 2015. The EMBL-EBI bioinformatics web and
668 programmatic tools framework. Nucleic Acids Res. 43, W580-W584.

669 Linger, J.G., Vardon, D.R., Guarnieri, M.T., Karp, E.M., Hunsinger, G.B., Franden,
670 M.A., Johnson, C.W., Chupka, G., Strathmann, T.J., Pienkos, P.T., Beckham,
671 G.T., 2014. Lignin valorization through integrated biological funneling and
672 chemical catalysis. Proc. Natl. Acad. Sci. U. S. A. 111, 12013-12018.
673 Masai, E., Ichimura, A., Sato, Y., Miyauchi, K., Katayama, Y., Fukuda, M., 2003. Roles
674 of the enantioselective glutathione *S*-transferases in cleavage of β-aryl ether. J.
675 Bacteriol. 185, 1768-1775.
676 Masai, E., Katayama, Y., Fukuda, M., 2007. Genetic and biochemical investigations on
677 bacterial catabolic pathways for lignin-derived aromatic compounds. Biosci.
678 Biotechnol. Biochem. 71, 1-15.
679 Masai, E., Shinohara, S., Hara, H., Nishikawa, S., Katayama, Y., Fukuda, M., 1999.
680 Genetic and biochemical characterization of a 2-pyrone-4,6-dicarboxylic acid
681 hydrolase involved in the protocatechuate 4,5-cleavage pathway of
682 *Sphingomonas paucimobilis* SYK-6. J. Bacteriol. 181, 55-62.
683 Meux, E., Prosper, P., Masai, E., Mulliert, G., Dumarçay, S., Morel, M., Didierjean, C.,
684 Gelhaye, E., Favier, F., 2012. *Sphingobium* sp. SYK-6 LigG involved in lignin
685 degradation is structurally and biochemically related to the glutathione
686 transferase omega class. FEBS Lett. 586, 3944-3950.
687 Michinobu, T., Bito, M., Yamada, Y., Tanimura, M., Katayama, Y., Masai, E.,
688 Nakamura, M., Otsuka, Y., Ohara, S., Shigehara, K., 2009. Fusible, elastic, and
689 biodegradable polyesters of 2-pyrone-4,6-dicarboxylic acid (PDC). Polym. J. 41,
690 1111-1116.
691 Ohta, Y., Hasegawa, R., Kurosawa, K., Maeda, A.H., Koizumi, T., Nishimura, H.,
692 Okada, H., Qu, C., Saito, K., Watanabe, T., Hatada, Y., 2017. Enzymatic
693 specific production and chemical functionalization of phenylpropanone platform
694 monomers from lignin. ChemSusChem. 10, 425-433.
695 Otsuka, Y., Nakamura, M., Shigehara, K., Sugimura, K., Masai, E., Ohara, S.,
696 Katayama, Y., 2006. Efficient production of 2-pyrone 4,6-dicarboxylic acid as a
697 novel polymer-based material from protocatechuate by microbial function. Appl.
698 Microbiol. Biotechnol. 71, 608-614.
699 Perez, J.M., Kontur, W.S., Alherech, M., Coplien, J., Karlen, S.D., Stahl, S.S.,
700 Donohue, T.J., Noguera, D.R., 2019. Funneling aromatic products of chemically
701 depolymerized lignin into 2-pyrone-4-6-dicarboxylic acid with

Novosphingobium aromaticivorans. Green Chem. 21, 1340-1350.

Qian, Y., Otsuka, Y., Sonoki, T., Mukhopadhyay, B., Nakamura, M., Masai, E., Katayama, Y., Okamura-Abe, Y., Jellison, J., Goodell, B., 2016. Engineered microbial production of 2-pyrone-4,6-dicarboxylic acid from lignin residues for use as an industrial platform chemical. Bioresources. 11, 6097-6109.

Ralph, J., Lundquist, K., Brunow, G., Lu, F., Kim, H., Schatz, P.F., Marita, J.M., Hatfield, R.D., Ralph, S.A., Christensen, J.H., Boerjan, W., 2004. Lignins: natural polymers from oxidative coupling of 4-hydroxyphenyl-propanoids. Phytochem. Rev. 3, 29-60.

Salis, H.M., Mirsky, E.A., Voigt, C.A., 2009. Automated design of synthetic ribosome binding sites to control protein expression. Nat. Biotechnol. 27, 946-950.

Sato, Y., Moriuchi, H., Hishiyama, S., Otsuka, Y., Oshima, K., Kasai, D., Nakamura, M., Ohara, S., Katayama, Y., Fukuda, M., Masai, E., 2009. Identification of three alcohol dehydrogenase genes involved in the stereospecific catabolism of arylglycerol-β-aryl ether by *Sphingobium* sp. strain SYK-6. Appl. Environ. Microbiol. 75, 5195-5201.

Scholten, J.D., Chang, K.H., Babbitt, P.C., Charest, H., Sylvestre, M., Dunaway-Mariano, D., 1991. Novel enzymic hydrolytic dehalogenation of a chlorinated aromatic. Science. 253, 182-185.

Shikinaka, K., Otsuka, Y., Nakamura, M., Masai, E., Katayama, Y., 2018. Utilization of lignocellulosic biomass via novel sustainable process. J. Oleo Sci. 67, 1059-1070.

Sievers, F., Wilm, A., Dineen, D., Gibson, T.J., Karplus, K., Li, W., Lopez, R., McWilliam, H., Remmert, M., Söding, J., Thompson, J.D., Higgins, D.G., 2011. Fast, scalable generation of high-quality protein multiple sequence alignments using Clustal Omega. Mol. Syst. Biol. 7, 539.

Song, F., Thoden, J.B., Zhuang, Z., Latham, J., Trujillo, M., Holden, H.M., Dunaway-Mariano, D., 2012. The catalytic mechanism of the hotdog-fold enzyme superfamily 4-hydroxybenzoyl-CoA thioesterase from *Arthrobacter* sp. strain SU. Biochemistry. 51, 7000-7016.

Song, F., Zhuang, Z., Dunaway-Mariano, D., 2007. Structure-activity analysis of base and enzyme-catalyzed 4-hydroxybenzoyl coenzyme A hydrolysis. Bioorg Chem. 35, 1-10.

Tanamura, K., Abe, T., Kamimura, N., Kasai, D., Hishiyama, S., Otsuka, Y., Nakamura, M., Kajita, S., Katayama, Y., Fukuda, M., Masai, E., 2011. Characterization of the third glutathione *S*-transferase gene involved in enantioselective cleavage of the β-aryl ether by *Sphingobium* sp. strain SYK-6. Biosci. Biotechnol. Biochem. 75, 2404-2407.

Yorifuji, T., Jeng, I.M., Barker, H.A., 1977. Purification and properties of 3-keto-5-aminohexanoate cleavage enzyme from a lysine-fermenting *Clostridium*. J. Biol. Chem. 252, 20-31.

Zakzeski, J., Bruijnincx, P.C.A., Jongerius, A.L., Weckhuysen, B.M., 2010. The catalytic valorization of lignin for the production of renewable chemicals. Chem. Rev. 110, 3552-3599.

Zhuang, Z., Gartemann, K.H., Eichenlaub, R., Dunaway-Mariano, D., 2003. Characterization of the 4-hydroxybenzoyl-coenzyme A thioesterase from *Arthrobacter* sp. strain SU. Appl. Environ. Microbiol. 69, 2707-2711.

Figure Legends

Fig. 1. Catabolic pathway of arylglycerol-β-aryl ether in *Sphingobium* sp. strain SYK-6 and the engineered pathway for production of PDC from HPV. The pathways for both guaiacyl (R = H)- and syringyl (R = OCH_3)-type β-aryl ether compounds are shown. The major pathway for the conversion of VAA into vanillate has not been identified. To construct an engineered strain capable of converting HPV into PDC, we employed the SYK-6 genes *vceA* and *vceB*, whose products convert VAA into vanilloyl-CoA and vanilloyl-CoA into vanillate, respectively. Enzyme genes for converting HPV into vanillate in pJHV01 (Fig. 5, Table S1) are shown in magenta. Enzyme genes for converting vanillate into PDC in pDVZ21 (Fig. 5, Table S1) are shown in green. Enzymes: LigD, LigL, and LigN, Cα-dehydrogenases; LigF, LigE, and LigP, β-etherases; LigG, glutathione *S*-transferase; HpvZ, HPV/HPS oxidase; ALDHs, aldehyde dehydrogenases; SLG_20400, VAL dehydrogenase; VceA, VAA/SAA-converting enzyme; VceB, vanilloyl-CoA/syringoyl-CoA thioesterase; LigM, vanillate/3-*O*-methylgallate *O*-demethylase; VanA and VanB, oxygenase and reductase components of vanillate *O*-demethylase; DesA, syringate *O*-demethylase; LigA and LigB, small and large subunits of protocatechuate 4,5-dioxygenase; LigC, CHMS dehydrogenase; DesZ, 3-*O*-methylgallate 3,4-dioxygenase. *Abbreviations*. GGE, guaiacylglycerol-β-guaiacyl ether; MPHPV, α-(2-methoxyphenoxy)-β-hydroxypropiovanillone; GS^-, reduced glutathione; GSSG, oxidized glutathione; GS-HPV, α-glutathionyl-β-hydroxypropiovanillone; HPV, β-hydroxypropiovanillone; HPS, β-hydroxypropiosyringone; VAL, vanilloyl acetaldehyde; SAL, 3-(4-hydroxy-3,5-dimethoxyphenyl)-3-oxopropanal; VAA, vanilloyl acetic acid; SAA, 3-(4-hydroxy-3,5-dimethoxyphenyl)-3-oxopropanoic acid; CoA, coenzyme A; CHMS, 4-carboxy-2-hydroxymuconate-6-semialdehyde; PDC, 2-pyrone-4,6-dicarboxylate.

Fig. 2. Characterization of SLG_24820 and SLG_24960 mutants. Enzyme activities of cell extracts of SYK-6, SLG_24820 mutant (Δ2482), and SLG_24960 mutant (Δ2496) toward VAA (A) and SAA (B). Cell extracts of SYK-6, Δ2482, and Δ2496 [200–1,000 μg protein/mL] were incubated with 100 μM VAA or SAA in the presence and absence of CoA [1 mM CoA + 1 mM ATP + 1.25 mM $MgSO_4$ (gray)], Ac-CoA [1 mM acetyl-CoA (white)], or Suc-CoA [1 mM succinyl-CoA (black)]. (C) Complementation of Δ2496 with pQF24960 carrying SLG_24960. Cell extracts of SYK-6(pQF), Δ2496(pQF), or Δ2496(pQF24960) [2–1,000 μg protein/mL] were incubated with VAA, respectively, in the presence of CoA, Ac-CoA, or Suc-CoA. All experiments were performed in triplicate, and each value represents the mean ± standard deviation. Asterisks indicate enzyme activity < 1.0 $nmol \cdot min^{-1} \cdot mg^{-1}$.

Fig. 3. Conversion of VAA by the cell extract of *E. coli* carrying SLG_24820 or SLG_24960. VAA (100 μM) was incubated with the cell extracts of *E. coli* harboring each of pET24960 (100 μg protein/mL; A and B) and pCold24820 (800 μg protein/mL; D, E) in the presence of 1 mM acetyl-CoA. Portions of the reaction mixtures were collected at the start (A and D), after 10 min (B), and after 2 h (E) of incubation and analyzed by HPLC–MS. The ESI–MS spectrum of Compound I (negative mode) is shown (C). (F) Chemical structure of Compound I (vanilloyl-CoA).

Fig. 4. Conversions of vanilloyl-CoA and syringoyl-CoA by the cell extract of *E. coli* carrying SLG_12450. VAA (100 μM; A and B) and SAA (100 μM; D and E) were incubated with VceA (1 μg protein/mL) plus a cell extract of *E. coli* BL21(DE3) harboring pET-16b (5 μg protein/mL). VAA and SAA (100 μM; C and F) were incubated with VceA (1 μg protein/mL) plus a cell extract of *E. coli* BL21(DE3) harboring pET12450 (5 μg protein/mL), respectively. Reactions were performed in the presence of 100 μM $CoSO_4$ and 1 mM acetyl-CoA. Portions of the reaction mixtures

were collected at the start (A and D) and after 30 min (B, C, E, and F) of incubation and analyzed by HPLC.

Fig. 5. Production of PDC from HPV by the engineered metabolic pathway constructed in *P. putida*. (A) Schematic representations of the *P. putida* PpY1100 recombinant strains, which contain pJB866 (vector) plus pDVZ21 or pJHV01 plus pDVZ21. Genes: *hpvZ*, HPV/HPS oxidase gene; SLG_20400, VAL dehydrogenase gene; *vceA*, VAA/SAA-converting enzyme gene; *vceB*, vanilloyl-CoA/syringoyl-CoA thioesterase gene; *vanA* and *vanB*, oxygenase and reductase component genes of vanillate *O*-demethylase; *ligA* and *ligB*, small and large subunit genes of protocatechuate 4,5-dioxygenase; *ligC*, CHMS dehydrogenase gene. (B) Conversion of 1 mM HPV by PpY1100(pJB866-pDVZ21) cells during growth in Wx medium containing 20 mM glucose. (C) Conversion of 1 mM HPV by PpY1100(pJHV01-pDVZ21) cells during growth in Wx medium containing 20 mM glucose. The concentrations of HPV (magenta), VAA (orange), vanillate (green), and PDC (cyan) were periodically measured by HPLC. Cell growth was measured by the OD_{600} (black). All experiments were performed in triplicate, and each value represents the mean ± standard deviation.

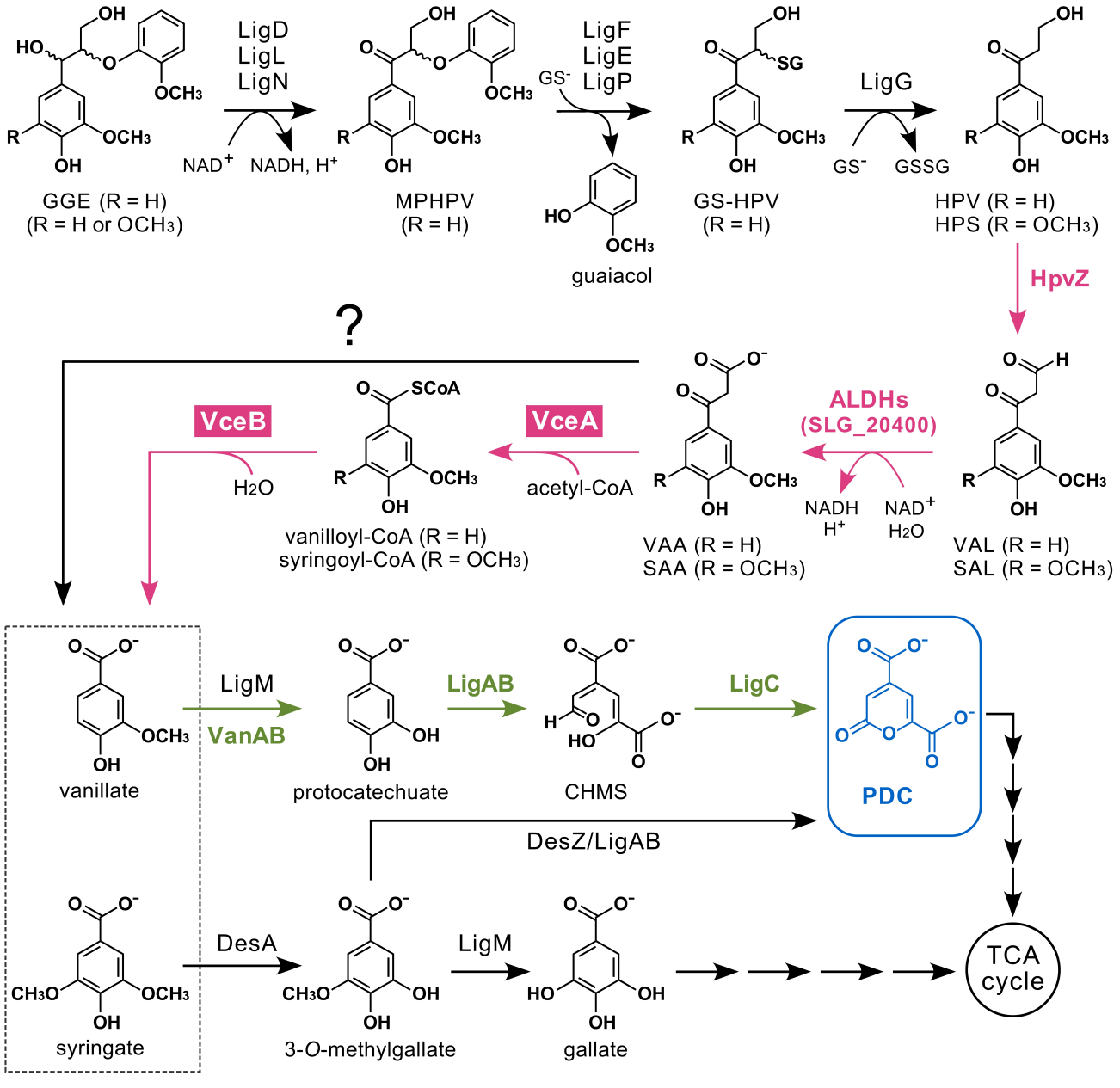
LigD
LigL
LigN
NAD+
NADH, H+
LigF
LigE
LigP
GS-
guaiacol
LigG
GS-
GSSG
GGE (R = H)
(R = H or OCH3)
MPHPV
(R = H)
GS-HPV
(R = H)
HPV (R = H)
HPS (R = OCH3)
HpvZ
?
VceB
H2O
VceA
acetyl-CoA
ALDHs
(SLG_20400)
NADH
H+
NAD+
H2O
vanilloyl-CoA (R = H)
syringoyl-CoA (R = OCH3)
VAA (R = H)
SAA (R = OCH3)
VAL (R = H)
SAL (R = OCH3)
LigM
VanAB
LigAB
LigC
vanillate
protocatechuate
CHMS
PDC
DesZ/LigAB
DesA
LigM
syringate
3-O-methylgallate
gallate
TCA
cycle

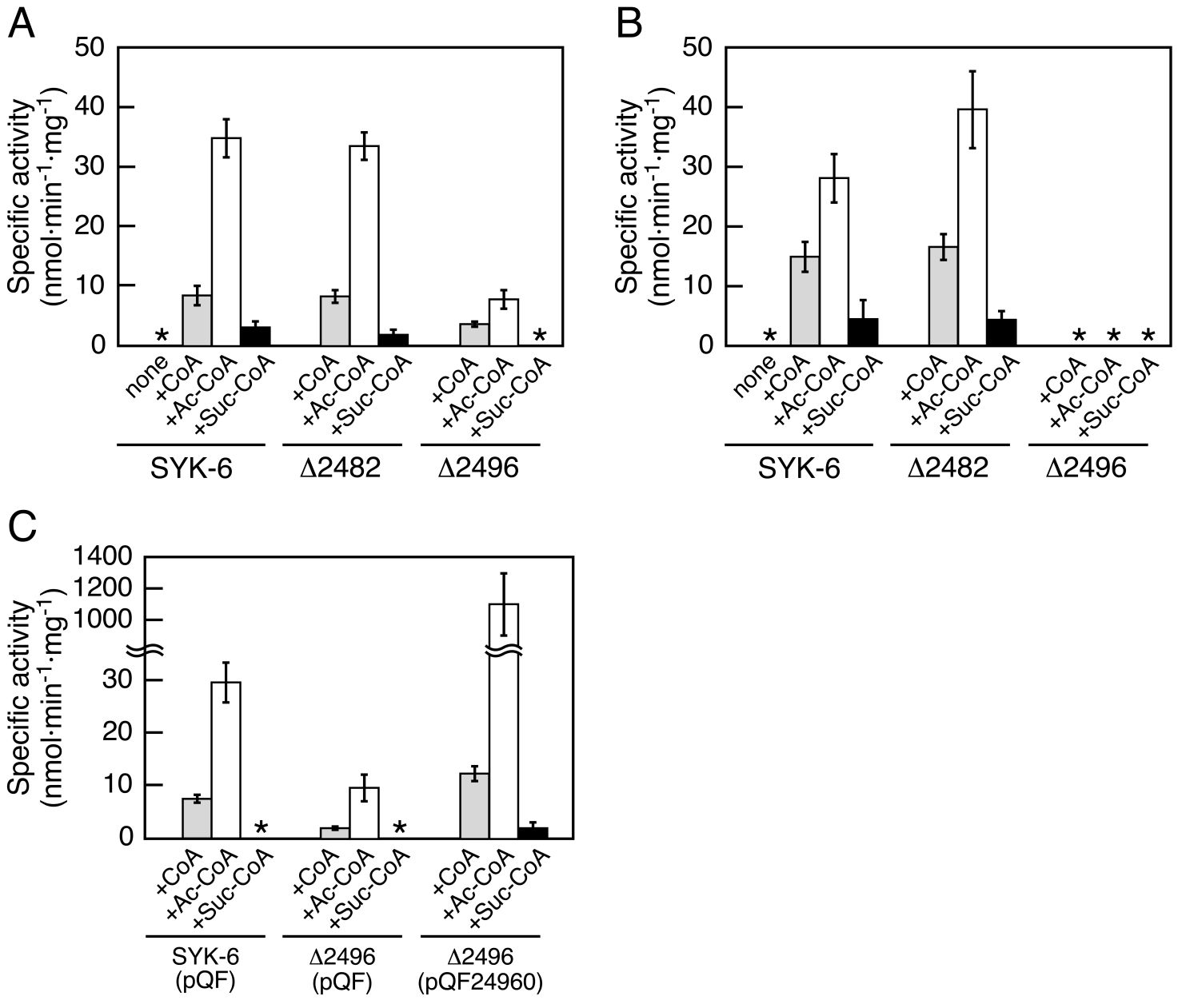
A
B
C
Specific activity
(nmol·min-1·mg-1)
50
40
30
20
10
0
1400
1200
1000
none
+CoA
+Ac-CoA
+Suc-CoA
SYK-6
Δ2482
Δ2496
SYK-6
(pQF)
Δ2496
(pQF)
Δ2496
(pQF24960)

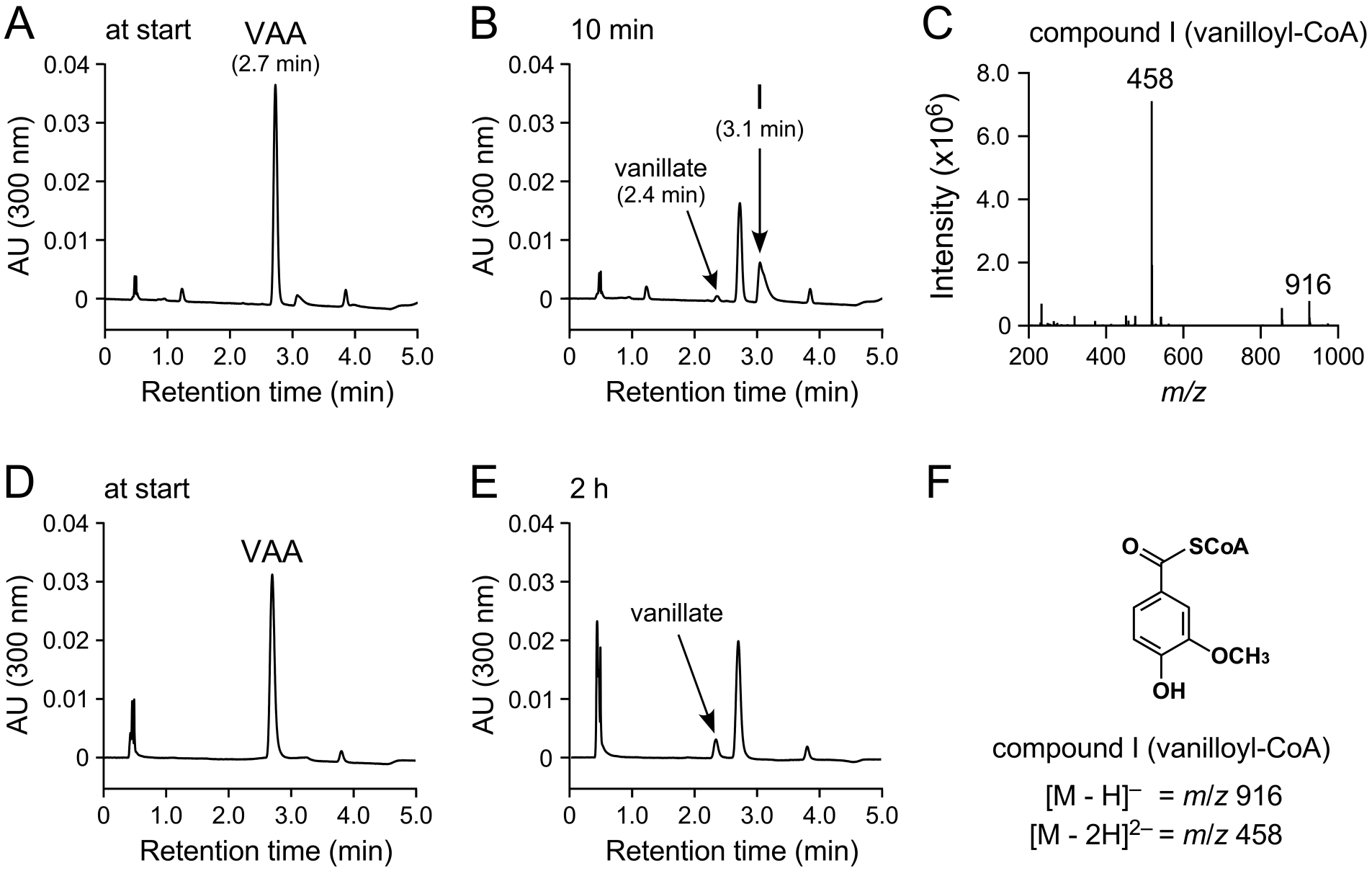
A
at start
VAA
(2.7 min)
AU (300 nm)
Retention time (min)
B
10 min
I
(3.1 min)
vanillate
(2.4 min)
C
compound I (vanilloyl-CoA)
458
916
Intensity (x10^6)
m/z
D
at start
VAA
E
2 h
vanillate
F
O
SCoA
OCH3
OH
compound I (vanilloyl-CoA)
[M - H]− = m/z 916
[M - 2H]2− = m/z 458

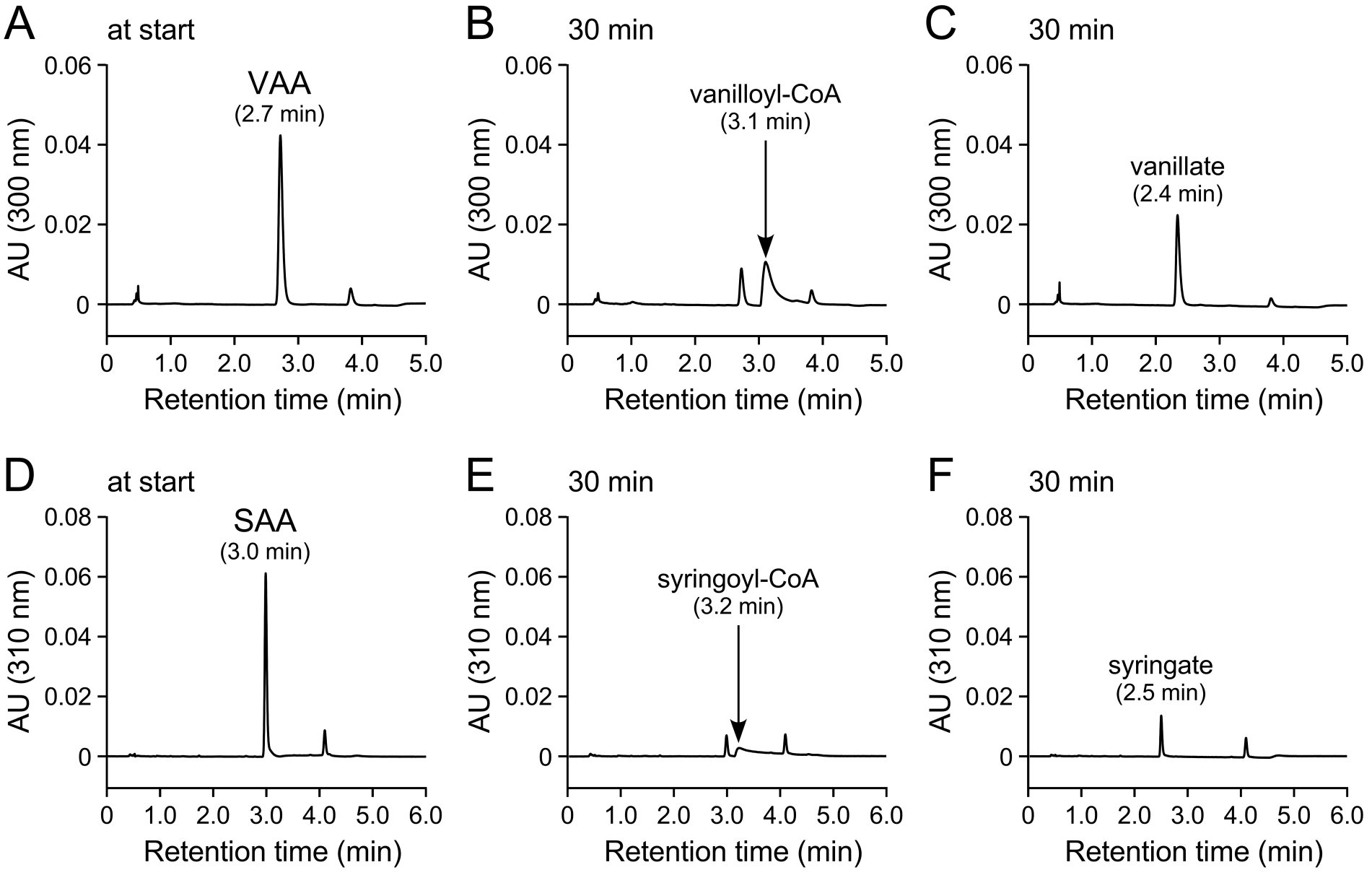
A
at start
VAA
(2.7 min)
AU (300 nm)
0.06
0.04
0.02
0
0
1.0
2.0
3.0
4.0
5.0
Retention time (min)
B
30 min
vanilloyl-CoA
(3.1 min)
AU (300 nm)
0.06
0.04
0.02
0
0
1.0
2.0
3.0
4.0
5.0
Retention time (min)
C
30 min
vanillate
(2.4 min)
AU (300 nm)
0.06
0.04
0.02
0
0
1.0
2.0
3.0
4.0
5.0
Retention time (min)
D
at start
SAA
(3.0 min)
AU (310 nm)
0.08
0.06
0.04
0.02
0
0
1.0
2.0
3.0
4.0
5.0
6.0
Retention time (min)
E
30 min
syringoyl-CoA
(3.2 min)
AU (310 nm)
0.08
0.06
0.04
0.02
0
0
1.0
2.0
3.0
4.0
5.0
6.0
Retention time (min)
F
30 min
syringate
(2.5 min)
AU (310 nm)
0.08
0.06
0.04
0.02
0
0
1.0
2.0
3.0
4.0
5.0
6.0
Retention time (min)

A

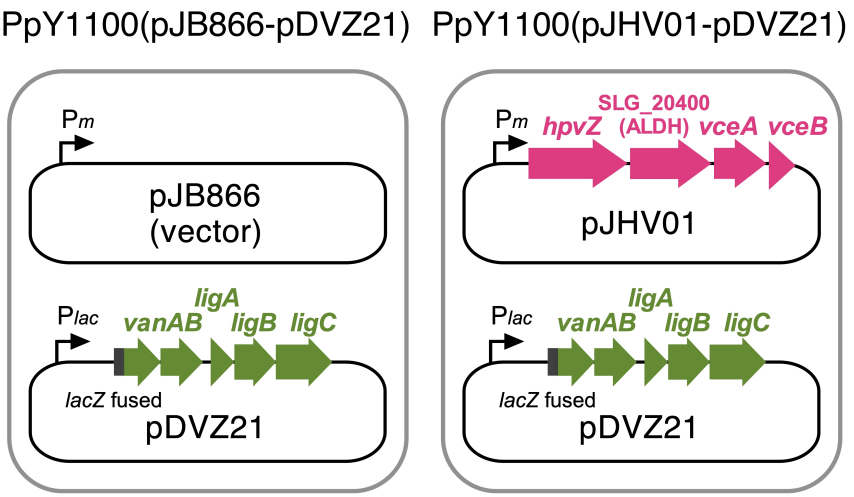
PpY1100(pJB866-pDVZ21)
PpY1100(pJHV01-pDVZ21)
Pm
pJB866
(vector)
Plac
ligA
vanAB
ligB
ligC
lacZ fused
pDVZ21
Pm
SLG_20400
hpvZ
(ALDH)
vceA
vceB
pJHV01
Plac
ligA
vanAB
ligB
ligC
lacZ fused
pDVZ21

B

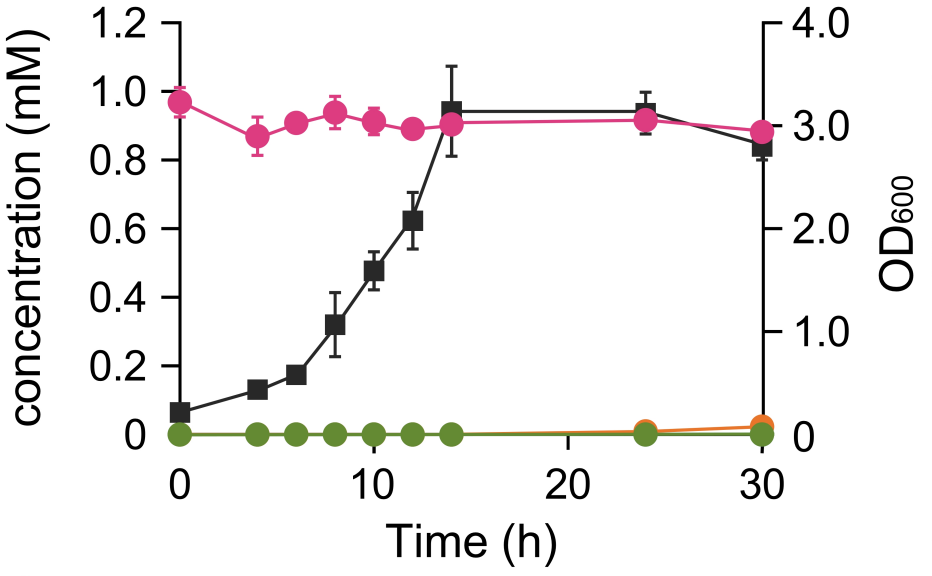
concentration (mM)
1.2
1.0
0.8
0.6
0.4
0.2
0
4.0
3.0
2.0
1.0
0
OD600
0
10
20
30
Time (h)

C

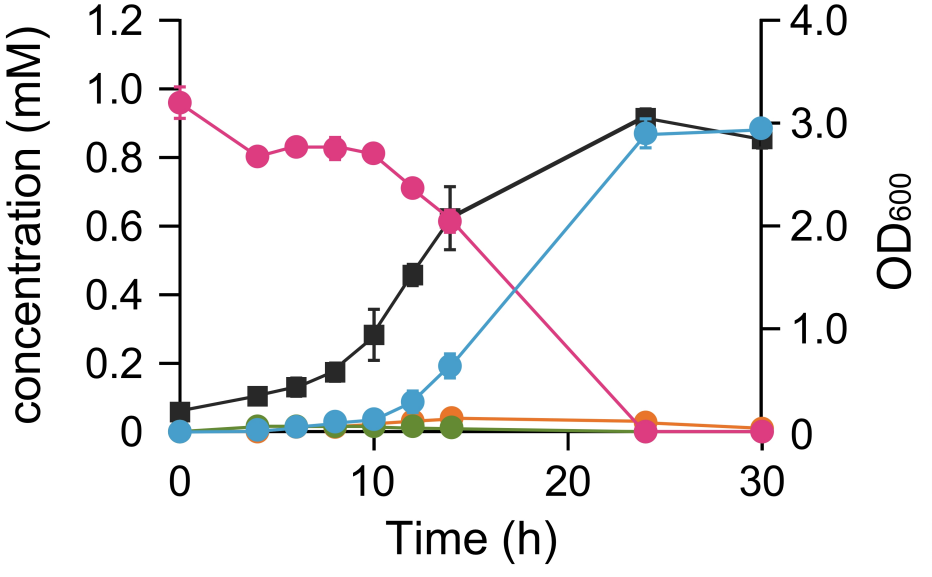
concentration (mM)
1.2
1.0
0.8
0.6
0.4
0.2
0
4.0
3.0
2.0
1.0
0
OD600
0
10
20
30
Time (h)

Supplemental materials

Table S1. Strains and plasmids used in this study

Strain or plasmid	Relevant characteristic(s)[a]	Reference or source
Strains		
Sphingobium sp.		
SYK-6	Wild type; Nal^r Sm^r	(Katayama et al., 1987)
Δ2482	SYK-6 derivative; ΔSLG_24820; Nal^r Sm^r	This study
Δ2496	SYK-6 derivative; ΔSLG_24960; Nal^r Sm^r	This study
Δ1245	SYK-6 derivative; ΔSLG_12450; Nal^r Sm^r	This study
Sphingobium japonicum		
UT26S	Nal^r	(Senoo and Wada, 1989)
Pseudomonas putida		
PpY1100	Nal^r Sm^r	(Katayama et al., 1987)
Escherichia coli		
BL21(DE3)	F$^-$ *ompT hsdS*$_B$(r_B^- m_B^-) *gal dcm* (DE3); T7 RNA polymerase gene under the control of the *lacUV5* promoter	(Studier and Moffatt, 1986)
HB101	*recA13 supE44 hsd20 ara-14 proA2 lacY1 galK2 rpsL20 xyl-5 mtl-1*	(Bolivar and Backman, 1979)
NEB 10-beta	Δ(*ara-leu*) *7697 araD139 fhuA* Δ*lacX74 galK16 galE15 e14- ϕ80*Δ*lacZ*Δ*M15 recA1 relA1 endA1 nupG rpsL* (Sm^r) *rph spoT1* Δ(*mrr-hsdRMS-mcrBC*)	New England Biolabs
Plasmids		
pVK100	Broad-host-range cosmid vector; Km^r Tc^r	(Ditta et al., 1980)
pRK2013	Tra$^+$ Mob$^+$ ColE1 replicon; Km^r	(Figurski and Helinski, 1979)
pBluescript II KS(+)	Cloning vector; Ap^r	(Short et al., 1988)
pET-16b	Expression vector; T7 promoter, Ap^r	Novagen
pCold I	Expression vector; *cspA* promoter, Ap^r	Takara Bio
pAK405	Plasmid for allelic exchange and markerless gene deletions in Sphingomonads; Km^r	(Kaczmarczyk et al., 2012)
pQF	Expression vector; P_{Q5} high-GC-content codon-optimized *cymR*, Tc^r	(Kaczmarczyk et al., 2013)
pJB866	RK2 broad-host-range expression vector; P_m *xylS*, Tc^r	(Blatny et al., 1997)
pCold12830	pCold I with a 1.7-kb NdeI-BamHI fragment carrying *hpvZ*	(Higuchi et al., 2018)
pT21-2040	pET-21a(+) with a 1.5-kb NdeI-BamHI fragment carrying SLG_20400	(Kamimura et al., 2017)
pDVZ21	pKT230MC carrying *ligABC* and *vanAB* from SYK-6 and *P. putida* PpY101, respectively	(Qian et al., 2016)
pVA17	pVK100 with partially SalI-digested fragments of SYK-6 carrying SLG_24820	This study
pVA116	pVK100 with partially SalI-digested fragments of SYK-6 carrying SLG_24820	This study
pET24820	pET-16b with a 0.9-kb NdeI-BamHI PCR amplified fragment carrying SLG_24820	This study
pET24960	pET-16b with a 0.9-kb NdeI-BamHI PCR amplified fragment carrying *vceA*	This study
pET12450	pET-16b with a 0.5-kb NdeI-BamHI PCR amplified fragment carrying *vceB*	This study
pCold24820	pCold I with a 0.9-kb NdeI-BamHI fragment carrying SLG_24820 from pET24820	This study
pAK24820	pAK405 with a 2.1-kb deletion cassette carrying up- and downstream regions of SLG_24820	This study
pAK24960	pAK405 with a 2.3-kb deletion cassette carrying up- and downstream regions of *vceA*	This study
pAK12450	pAK405 with a 2.1-kb deletion cassette carrying up- and downstream regions of *vceB*	This study
pQF24960	pQF with a 0.9-kb HindIII-EcoRI PCR amplified fragment carrying *vceA*	This study
pJHV01	pJB866 with a 4.6-kb BamHI PCR amplified fragment carrying *hpvZ*, SLG_20400, *vceA*, and *vceB*	This study

[a]Nal^r, Sm^r, Km^r, Tc^r, and Ap^r, resistance to nalidixic acid, streptomycin, kanamycin, tetracycline, and ampicillin, respectively.

Table S2. Primers used in this study

Gene, plasmid, or strain	Primer	Sequence (5′ to 3′)
Amplification of *vceA* and its homologs		
SLG_12200	12200_amp_F	TCGAAGGTCGTCATATGCGCCGCTCGAAGAAA
	12200_amp_R	GTTAGCAGCCGGATCCTCAGAAGCCGACGCGGTC
SLG_14250	14250_amp_F	TCGAAGGTCGTCATATGCTCGCTGGGAATAAGA
	14250_amp_R	GTTAGCAGCCGGATCCTCAGGCCGCCTTGAGCCC
SLG_24820	24820_exp_F	TCGAAGGTCGTCATATGAGCAATCGCCGCATG
	24820_exp_R	GTTAGCAGCCGGATCCTCAGACCGGATTCAGGCC
SLG_24960 (*vceA*)	24960_exp_F	TCGAAGGTCGTCATATGGCCAAGACCTTCATCA
	24960_exp_R	GTTAGCAGCCGGATCCTCAGCCCTTGAGGCCGAG
Construction of plasmids		
pET24820	24820_exp_F	TCGAAGGTCGTCATATGAGCAATCGCCGCATG
	24820_exp_R	GTTAGCAGCCGGATCCTCAGACCGGATTCAGGCC
pET24960	24960_exp_F	TCGAAGGTCGTCATATGGCCAAGACCTTCATCA
	24960_exp_R	GTTAGCAGCCGGATCCTCAGCCCTTGAGGCCGAG
pET12450	12450_exp_F	TCGAAGGTCGTCATATGACCGACGAGCCGCGC
	12450_exp_R	GTTAGCAGCCGGATCCTCAGGCAGCGGAGCCGAA
pAK24820	dis24820_top_F	CGGTACCCGGGGATCAGCGGTTGAAGGAGATCGGC
	dis24820_top_R	GCTTCTCTCCTGACTGCGTA
	dis24820_bot_F	TACGCAGTCAGGAGAGAAGCGGATGCCCCTCCCCGCCGGA
	dis24820_bot_R	CGACTCTAGAGGATCGTCGAGGAGAGGACGAAGCC
pAK24960	dis24960_top_F	CGGTACCCGGGGATCCGATGACTGGGATCGTGCCT
	dis24960_top_R	GTTATCGCTCTCCTGTGATT
	dis24960_bot_F	AATCACAGGAGAGCGATAACGCGACGGCGCATTGCCGGGA
	dis24960_bot_R	CGACTCTAGAGGATCGGACGGCAAGCCATATAGTG
pAK12450	dis12450_top_F	CGGTACCCGGGGATCTATCGACCTTTACTACATGC
	dis12450_top_R	GGGGCGAAATCCAGTCCGCC
	dis12450_bot_F	GGCGGACTGGATTTCGCCCCGACCGATGGCGCGGGACCAG
	dis12450_bot_R	CGACTCTAGAGGATCGATACCGAAATTGAGGCTGA
pQF24960	pQF24960_F	CTAGTAGAGGAAGCTATGGCCAAGACCTTCATCAC
	pQF24960_R	TCACTTCACCGGATCTCAGCCCTTGAGGCCGAGCA
pJHV01	pJHV01_12830_F	TGACGTCACCATGGGAAGCTTCGTGACGCACAAGACAAAATTT AAGGAGGTATATTGTAAATGGTTGATGTCAGAACGGT
	pJHV01_12830_R	TCAGGCGGGCGCCAGTTCCT
	pJHV01_20400_F	CGCGAAGGAACTGGCGCCCGCCTGAGCAGGCGCCTACACATT ATTAAGGAGGTATTTTTATGACCAGCTCCACGCAGAA
	pJHV01_20400_R	TCAGGCGGCAGCGTGCTGAT
	pJHV01_24960_F	CCTGCATCAGCACGCTGCCGCCTGACTCATCCGCGGGCTACCA ATTACGTTCACAAGCGTAACCACAATATTTAAGGAGGATTTTT TTATGGCCAAGACCTTCATCAC
	pJHV01_24960_R	TCAGCCCTTGAGGCCGAGCA

	pJHV01_12450_F	CGAGATGCTCGGCCTCAAGGGCTGATCGGTAAGCCGTCTCGCG CCTGGGGTAAAACGAACCCAATAAGGAGGTTTTTTTTATGACC GACGAGCCGCGCGC
	pJHV01_12450_R	TCGAGGAATTCCTGCAGGATATCTGTCAGGCAGCGGAGCCGA ACA
Colony PCR		
Δ2482	dis24820_conf_F	ATCCACCAGCAGATCCTCGT
	dis24820_bot_R	CGACTCTAGAGGATCGTCGAGGAGAGGACGAAGCC
Δ2496	dis24960_conf_F	TATCACATGGCGATGCAGGC
	dis24960_bot_R	CGACTCTAGAGGATCGGACGGCAAGCCATATAGTG
Δ1245	dis12450_conf_F	TCATCTGGCGAGCAAGTGCG
	dis12450_bot_R	CGACTCTAGAGGATCGATACCGAAATTGAGGCTGA

Table S3. Metal ion dependency of VceA

Metal ion	Specific activity[a] ($\mu mol \cdot min^{-1} \cdot mg^{-1}$)
None	2.0 ± 0.1
Zn^{2+}	0.94 ± 0.12
Fe^{2+}	2.2 ± 0.3
Mg^{2+}	1.8 ± 0.3
Mn^{2+}	9.5 ± 0.6
Ca^{2+}	1.9 ± 0.2
Cu^{2+}	0.36 ± 0.05
Co^{2+}	17.4 ± 3.8
Mo^{2+}	1.9 ± 0.3

[a]Purified VceA (1–5 μg protein/mL) was incubated with 100 μM VAA in the presence of 1 mM acetyl-CoA and 100 μM of each metal ion. Each value represents the mean ± standard deviation of three independent experiments.

Table S4. CoA donor specificity of VceA

CoA donor	Specific activity[a] ($\mu mol \cdot min^{-1} \cdot mg^{-1}$)
CoA	ND
acetyl-CoA	17.4 ± 3.8 (100)
propionyl-CoA	5.67 ± 0.03 (33)
butyryl-CoA	0.19 ± 0.14 (1)
malonyl-CoA	0.084 ± 0.005 (<1)
acetoacetyl-CoA	0.13 ± 0.02 (<1)
succinyl-CoA	ND
benzoyl-CoA	ND

[a]Purified VceA (1–50 μg protein/mL) was incubated with 100 μM VAA in the presence of 100 μM $CoSO_4$ and each 1 mM CoA donor. Each value represents the mean ± standard deviation of three independent experiments. ND, not detected. Numbers in parentheses indicate the relative activity.

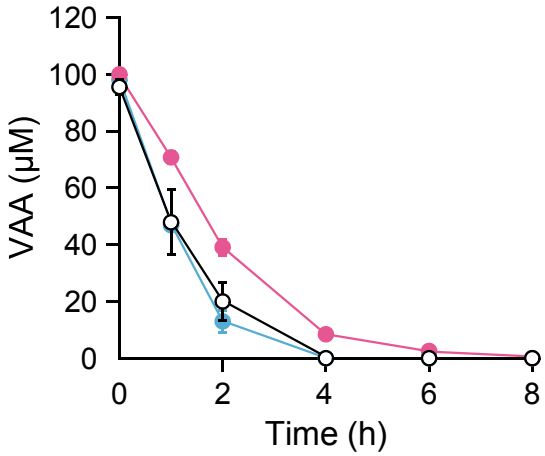

Fig. S1. Inducibility of VAA conversion in SYK-6.

Resting cells (OD_{600} = 2.0) of SYK-6 grown in Wx-SEMP (white), Wx-SEMP + 2 mM GGE (cyan), and Wx-SEMP + 2 mM HPV (magenta) were incubated with 100 μM VAA. Portions of the reaction mixtures were collected, and the amount of VAA was measured by HPLC. All experiments were performed in triplicate, and each value represents the mean ± standard deviation.

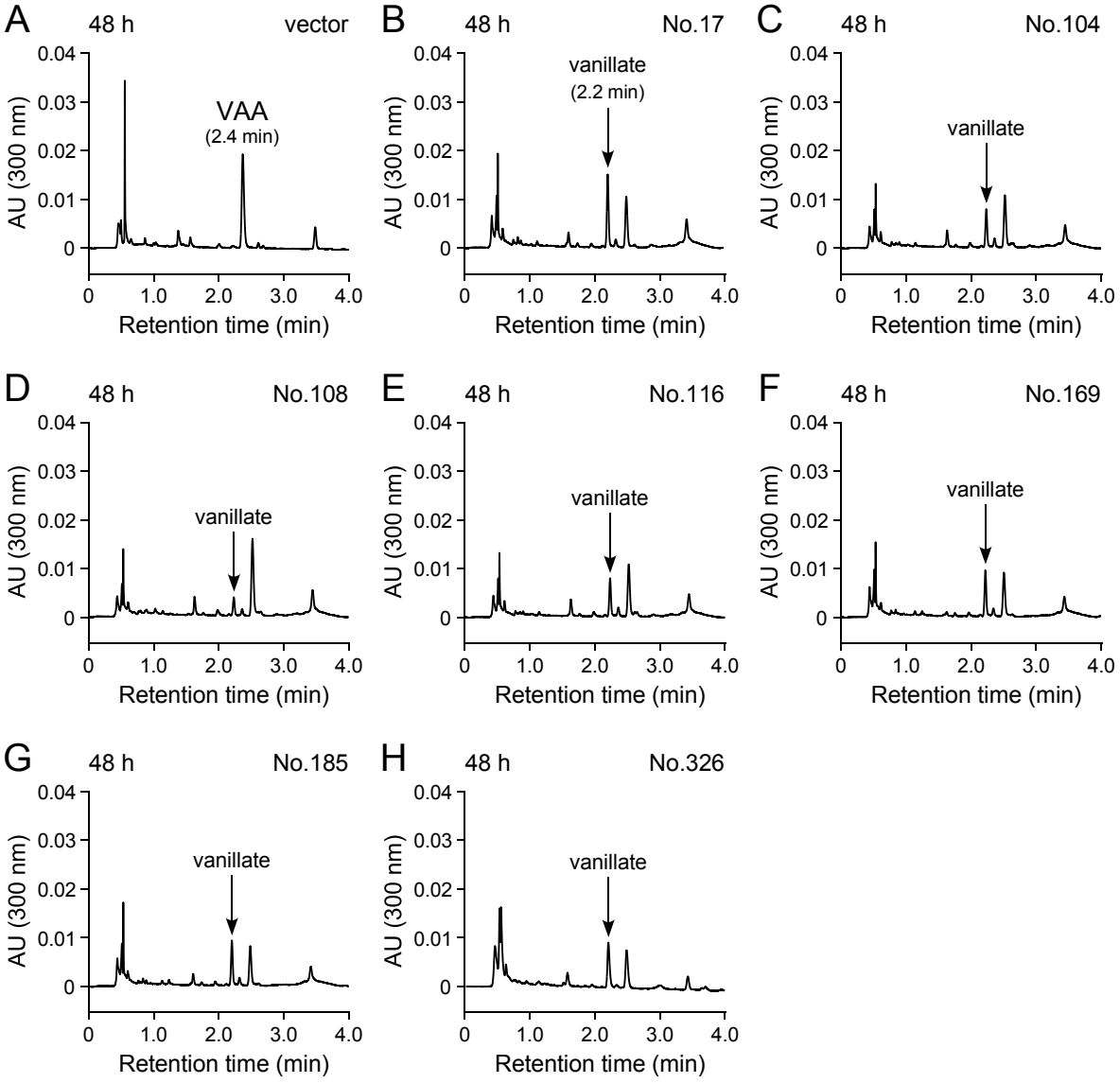

Fig. S2. Conversion of VAA into vanillate by the seven isolated transconjugants.

VAA (50 μM) was incubated with cells of *S. japonicum* UT26S harboring pVK100 (A; vector) and transconjugants that showed the ability to convert VAA (B–H). Portions of the reaction mixtures were collected after 48 h of incubation and analyzed by HPLC.

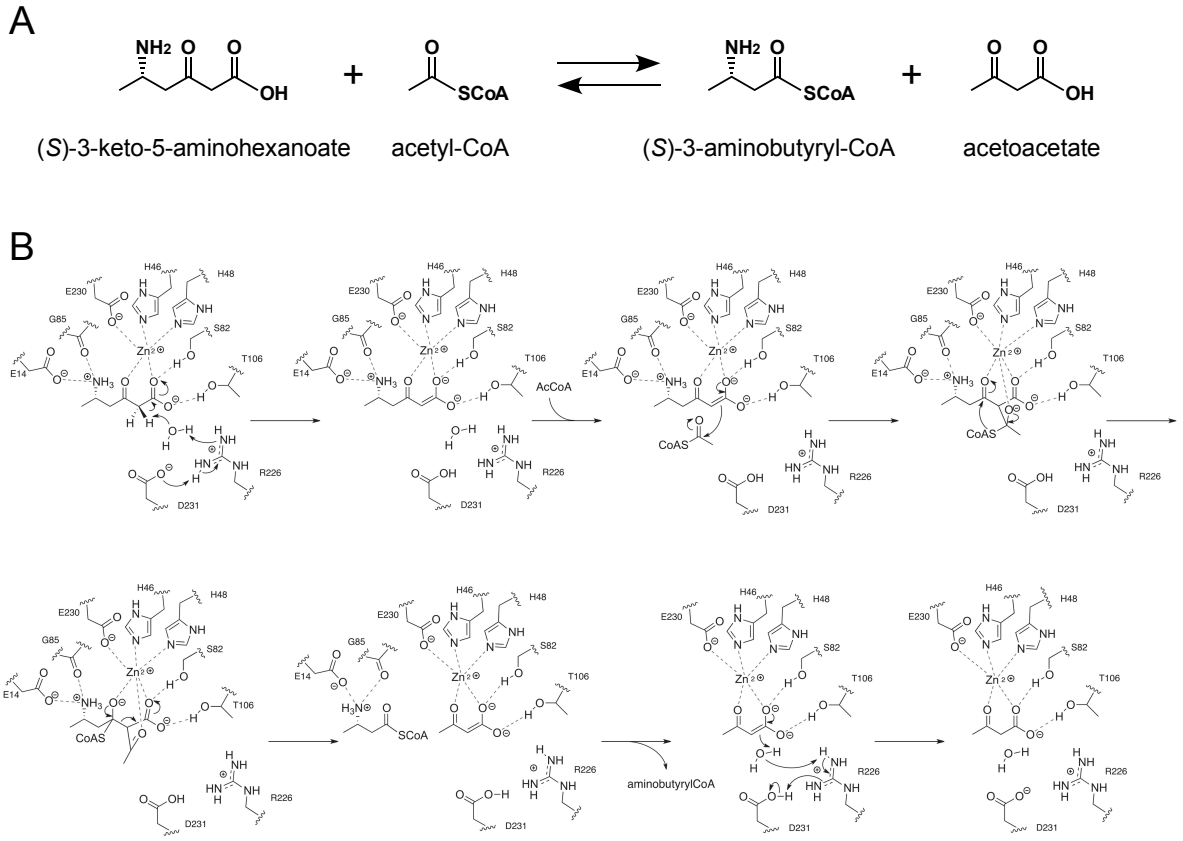

Fig. S3. Reaction of the 3-keto-5-aminohexanoate cleavage enzyme (Kce).

(A) Reaction scheme of Kce. (B) A schematic representation of the course of the Kce reaction. Figures are reproduced from (Bellinzoni et al., 2011) under the Creative Commons (CC-NC-BY) license.

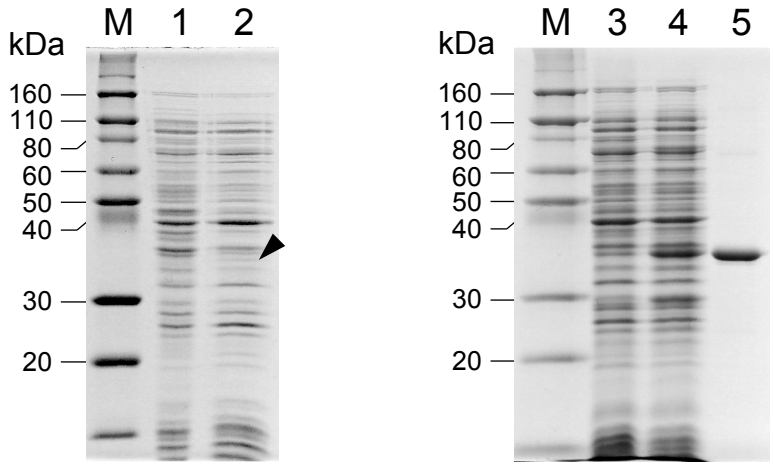

Fig. S4. Expression of SLG_24820 and SLG_24960 in *E. coli* and purification of the gene product of SLG_24960.

Proteins were separated on SDS-12% polyacrylamide gels and stained with Coomassie Brilliant Blue. Lanes: 1, *E. coli* BL21(DE3) harboring pCold I (vector); 2, *E. coli* BL21(DE3) harboring pCold24820; 3, *E. coli* BL21(DE3) harboring pET-16b (vector); 4 and 5, *E. coli* BL21(DE3) harboring pET24960; 1–4, cell extracts (10 μg); 5, purified enzyme (1 μg); M, molecular mass markers.

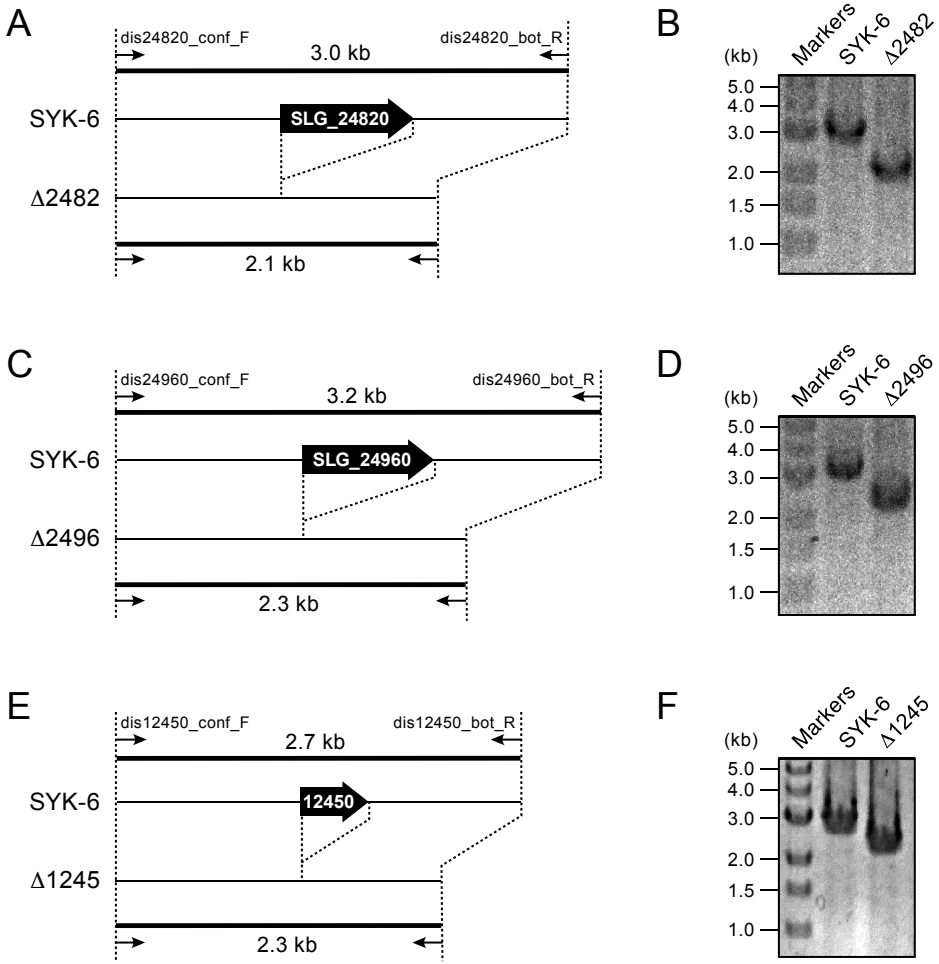

Fig. S5. Disruption of SLG_24820, SLG_24960, and SLG_12450 in SYK-6.

Schematic representations of the disruption of SLG_24820 (A), SLG_24960 (*vceA*; C), and SLG_12450 (*vceB*; E) by deletion. (B, D, F) Colony PCR analysis of mutants using primer pairs of dis24820_conf_F–dis24820_bot_R (B), dis24960_conf_F–dis24960_bot_R (D), and dis12450_conf_F–dis12450_bot_R (F) (Table S2).

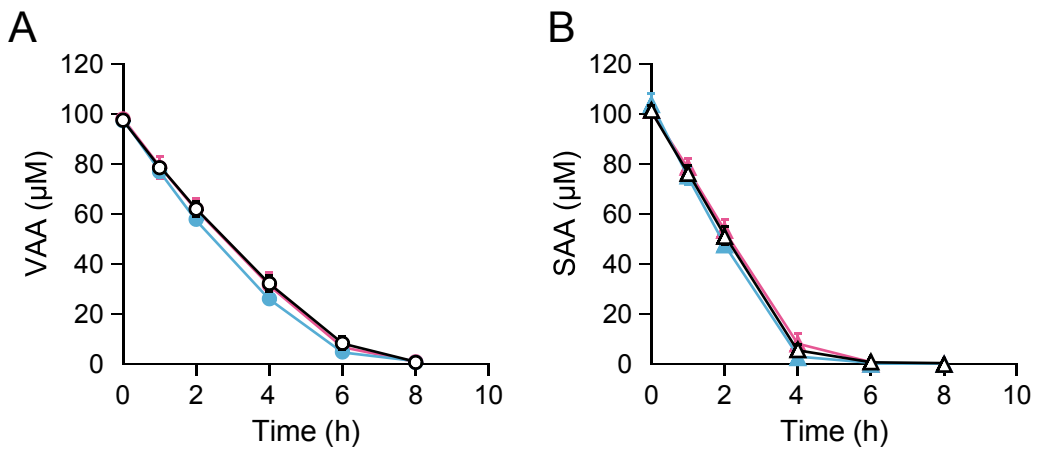

Fig. S6. Conversion of VAA and SAA by SYK-6, Δ2482, and Δ2496 resting cells.

Resting cells (OD_{600} = 0.5) of SYK-6 (white), Δ2482 (cyan), and Δ2496 (magenta) were incubated with 100 μM VAA (A) and SAA (B). Portions of the reaction mixtures were collected, and the amounts of VAA and SAA were measured by HPLC. All experiments were performed in triplicate, and each value represents the mean ± standard deviation.

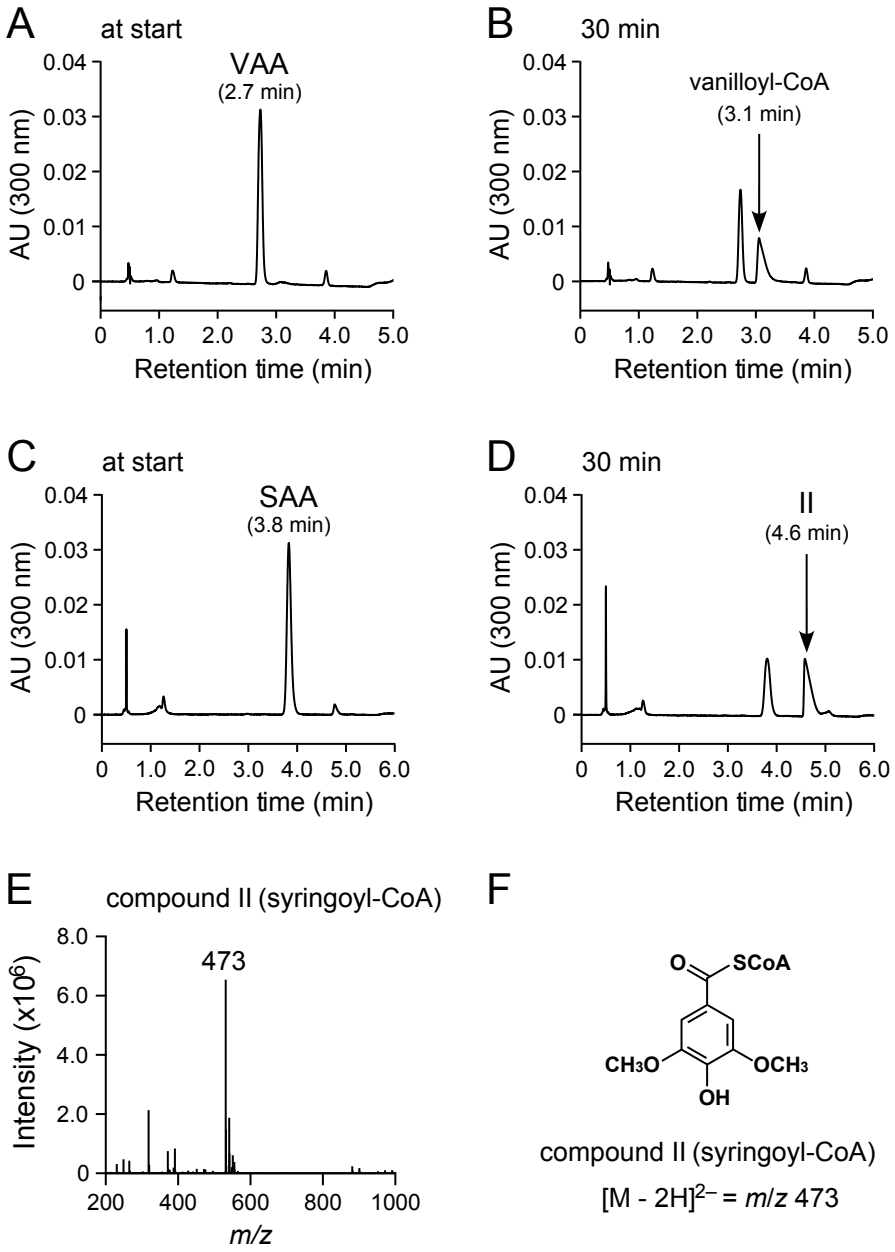

Fig. S7. Conversion of VAA and SAA by purified VceA.

VAA (100 µM; A and B) and SAA (100 µM; C and D) were incubated with VceA (10 µg protein/mL) in the presence of 200 µM acetyl-CoA. Portions of the reaction mixtures were collected at the start (A and C) and after 30 min of incubation (B and D) and then analyzed by HPLC–MS. (E) ESI–MS spectrum of Compound II (negative mode). (F) Chemical structure of Compound II (syringoyl-CoA).

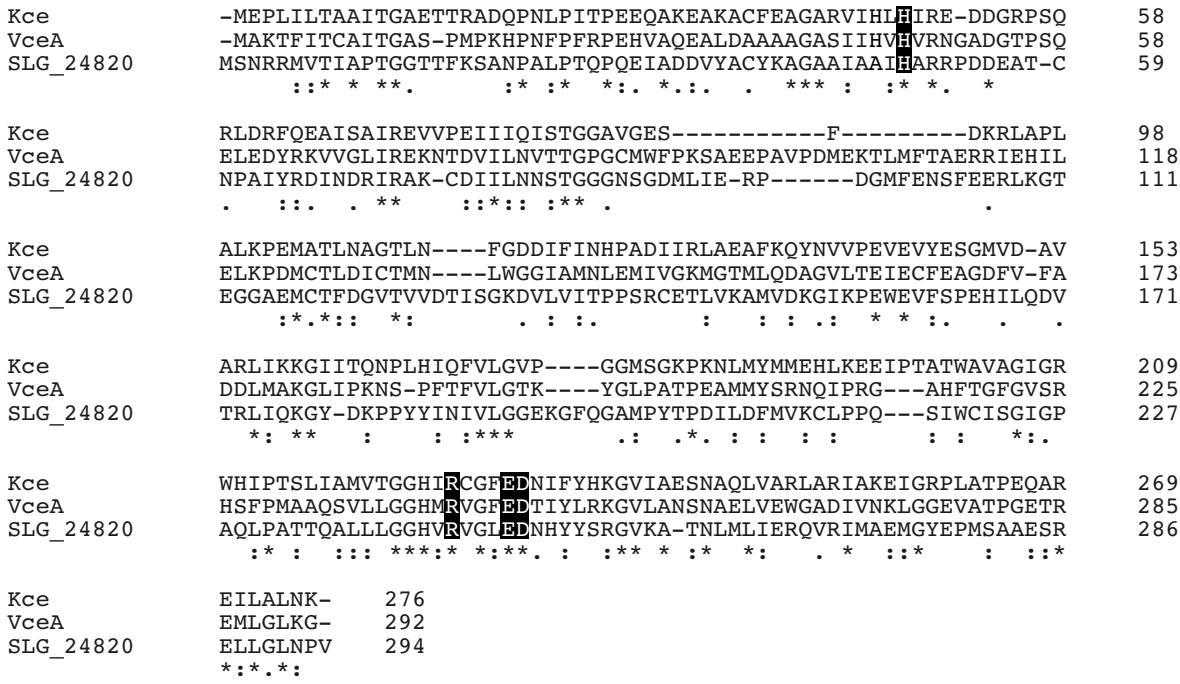

Fig. S8. Amino acid sequence alignment of Kce, VceA, and SLG_24820.
Residues highly conserved in DUF849-containing proteins are shown with a black background. The asterisks, colons, and periods indicate identical residues, conserved residues, and semiconserved residues, respectively.

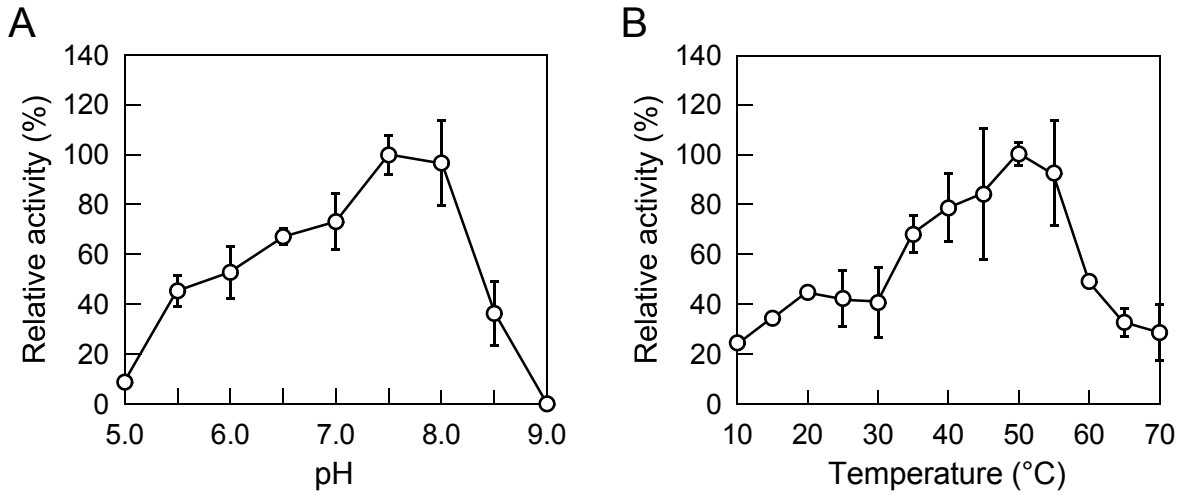

Fig. S9. Optimum pH (A) and temperature (B) for VceA.

(A) The enzyme activity of VceA for 100 μM VAA was determined using 50 mM GTA buffer (pH 5.0–9.0) at 30°C. (B) The enzyme activity of VceA for 100 μM VAA was determined using 50 mM Tris-HCl buffer (pH 7.5) at 10–70°C. Each value represents the mean ± standard deviation of three independent experiments.

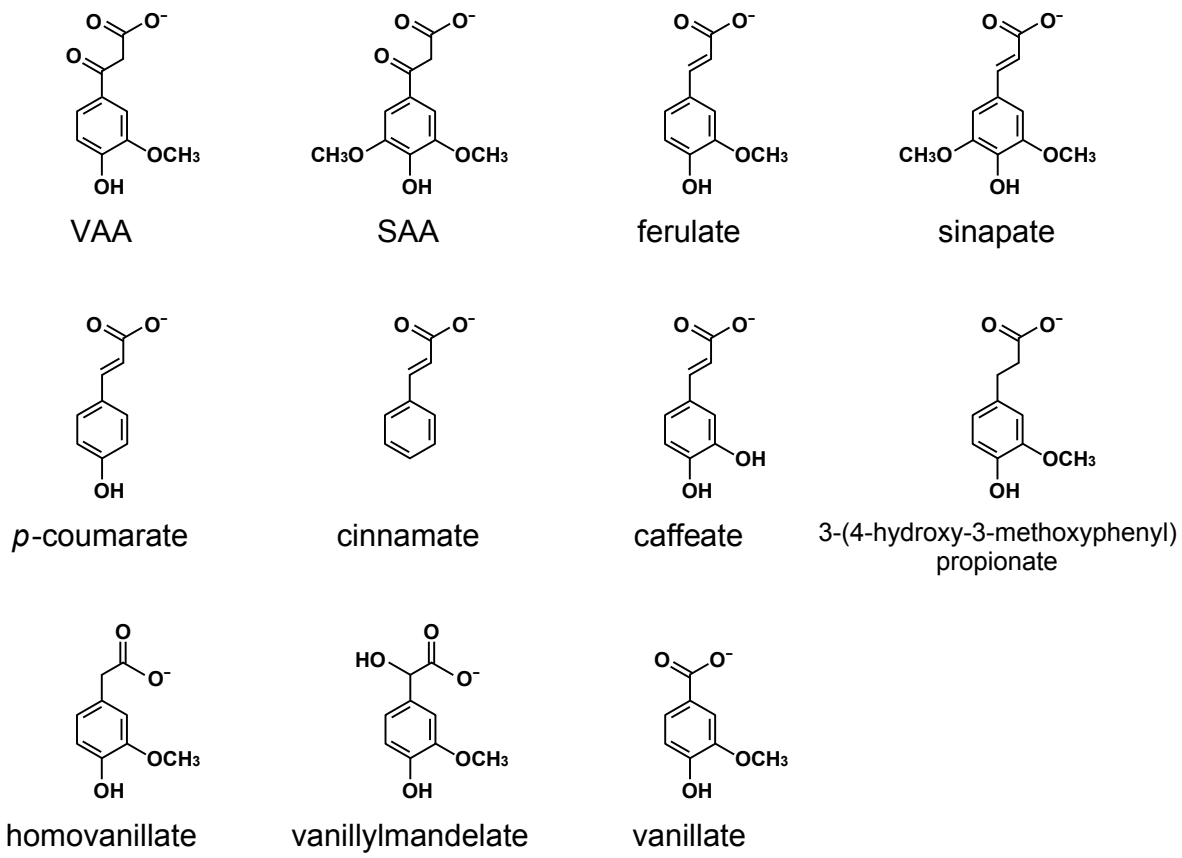

Fig. S10. Chemical structures of substrates used to examine the substrate range of VceA.
Abbreviations. VAA, vanilloyl acetic acid; SAA, 3-(4-hydroxy-3,5-dimethoxyphenyl)-3-oxopropanoic acid.

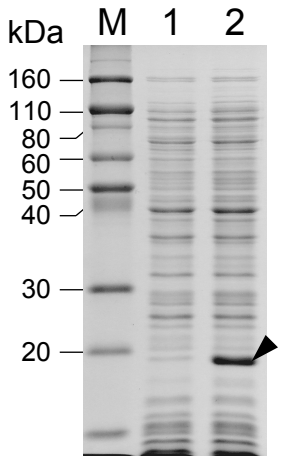

Fig. S11. Expression of SLG_12450 in *E. coli*.
Proteins (10 μg) were separated on an SDS-12% polyacrylamide gel and stained with Coomassie Brilliant Blue. Lanes: M, molecular mass markers; 1, cell extract of *E. coli* BL21(DE3) harboring pET-16b; 2, cell extract of *E. coli* BL21(DE3) harboring pET12450.

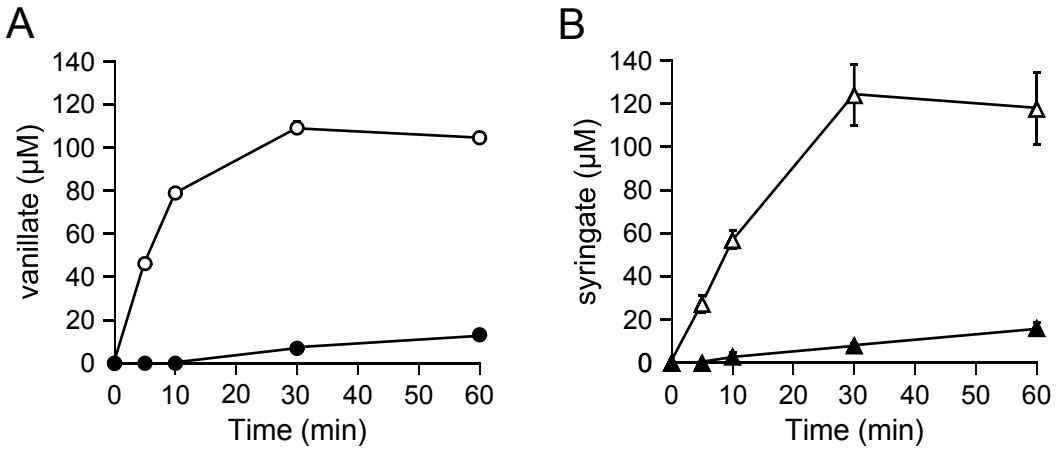

Fig. S12. Characterization of SLG_12450 mutant (Δ1245).

Time course of the production of vanillate (A) and syringate (B) during the incubation of VAA and SAA, respectively, with a cell extract of SYK-6 (open symbols; 20 μg protein/mL) or Δ1245 (closed symbols; 20 μg protein/mL) in the presence of VceA (10 μg protein/mL), 100 μM $CoSO_4$, and 1 mM acetyl-CoA. All experiments were performed in triplicate, and each value represents the mean ± standard deviation.

References

Bellinzoni, M., Bastard, K., Perret, A., Zaparucha, A., Perchat, N., Vergne, C., Wagner, T., de Melo-Minardi, R.C., Artiguenave, F., Cohen, G.N., Weissenbach, J., Salanoubat, M., Alzari, P.M., 2011. 3-Keto-5-aminohexanoate cleavage enzyme: a common fold for an uncommon Claisen-type condensation. J. Biol. Chem. 286, 27399-27405.

Blatny, J.M., Brautaset, T., Winther-Larsen, H.C., Karunakaran, P., Valla, S., 1997. Improved broad-host-range RK2 vectors useful for high and low regulated gene expression levels in gram-negative bacteria. Plasmid. 38, 35-51.

Bolivar, F., Backman, K., 1979. Plasmids of *Escherichia coli* as cloning vectors. Methods Enzymol. 68, 245-267.

Ditta, G., Stanfield, S., Corbin, D., Helinski, D.R., 1980. Broad host range DNA cloning system for gram-negative bacteria: construction of a gene bank of *Rhizobium meliloti*. Proc. Natl. Acad. Sci. U. S. A. 77, 7347-7351.

Figurski, D.H., Helinski, D.R., 1979. Replication of an origin-containing derivative of plasmid RK2 dependent on a plasmid function provided in *trans*. Proc. Natl. Acad. Sci. U. S. A. 76, 1648-1652.

Higuchi, Y., Aoki, S., Takenami, H., Kamimura, N., Takahashi, K., Hishiyama, S., Lancefield, C.S., Ojo, O.S., Katayama, Y., Westwood, N.J., Masai, E., 2018. Bacterial catabolism of β-hydroxypropiovanillone and β-hydroxypropiosyringone produced in the reductive cleavage of arylglycerol-β-aryl ether in lignin. Appl. Environ. Microbiol. 84, e02670-17.

Kaczmarczyk, A., Vorholt, J.A., Francez-Charlot, A., 2012. Markerless gene deletion system for Sphingomonads. Appl. Environ. Microbiol. 78, 3774-3777.

Kaczmarczyk, A., Vorholt, J.A., Francez-Charlot, A., 2013. Cumate-inducible gene expression system for Sphingomonads and other *Alphaproteobacteria*. Appl. Environ. Microbiol. 79, 6795-6802.

Kamimura, N., Goto, T., Takahashi, K., Kasai, D., Otsuka, Y., Nakamura, M., Katayama, Y., Fukuda, M., Masai, E., 2017. A bacterial aromatic aldehyde dehydrogenase critical for the efficient catabolism of syringaldehyde. Sci. Rep. 7, 44422.

Katayama, Y., Nishikawa, S., Nakamura, M., Yano, K., Yamasaki, M., Morohoshi, N., Haraguchi, T., 1987. Cloning and expression of *Pseudomonas paucimobilis* SYK-6 genes involved in the degradation of vanillate and protocatechuate in *P. putida*. Mokuzai Gakkaishi. 33, 77-79.

Qian, Y., Otsuka, Y., Sonoki, T., Mukhopadhyay, B., Nakamura, M., Masai, E., Katayama, Y., Okamura-Abe, Y., Jellison, J., Goodell, B., 2016. Engineered microbial production of 2-pyrone-4,6-dicarboxylic acid from lignin residues for use as an industrial platform chemical. Bioresources. 11, 6097-6109.

Senoo, K., Wada, H., 1989. Isolation and identification of an aerobic γ-HCH-decomposing bacterium from soil. Soil Sci. Plant Nutr. 35, 79-87.

Short, J.M., Fernandez, J.M., Sorge, J.A., Huse, W.D., 1988. λ ZAP: a bacteriophage λ expression vector with in vivo excision properties. Nucleic Acids Res. 16, 7583-7600.

Studier, F.W., Moffatt, B.A., 1986. Use of bacteriophage T7 RNA polymerase to direct selective high-level expression of cloned genes. J. Mol. Biol. 189, 113-130.